Treatment of Lung Cancer with an ALK Inhibitor After *EML4-ALK* Fusion Gene Detection Using Endobronchial Ultrasound-Guided Transbronchial Needle Aspiration

Takahiro Nakajima, MD, PhD,† Hideki Kimura, MD, PhD,* Kengo Takeuchi, MD, PhD,‡ Manabu Soda, MD, PhD,§ Hiroyuki Mano, MD, PhD,§ Kazuhiro Yasufuku, MD, PhD,† and Toshihiko Iizasa, MD, PhD**

A 40-year-old man who had complained of bloody sputum was referred to our hospital for workup. Chest computed tomography showed a significant mediastinal lymphadenopathy (Figure 1*A*). Bronchoscopic examination revealed a tumor compressing the right mainstem bronchus (Figure 2*A*). Massive bleeding from the tumor was caused by passage of the bronchoscope. Therefore, a diagnosis of pulmonary adenocarcinoma was made by sputum cytology. The patient first received conventional chemotherapy in the form of four courses of cisplatin plus vinorelbine (CDDP + VNR), two cycles of cisplatin plus gemcitabine (CDDP + GEM), and four cycles of carboplatin plus gemcitabine (CBDCA + GEM). However, both the size of the tumor and the serum carcinoembryonic antigen level continued to increase. Fluorodeoxyglucose positron emission tomography suggested systemic metastasis in hilar and mediastinal lymph nodes and bone (Figure 1*B*).

We performed endobronchial ultrasound-guided transbronchial needle aspiration (EBUS-TBNA) to avoid bleeding from the tumor. Metastatic adenocarcinoma was revealed in an upper paratracheal lymph node (#2R) (Figures 2*B*, *C*). Because the epidermal growth factor receptor gene was wild type, we examined the presence of ALK fusion genes. Immunohistochemistry by the intercalated antibody-enhanced polymer (iAEP) method[1] showed an expression of ALK protein in the samples obtained by EBUS-TBNA (Figure 2*D*). *EML4-ALK* fusion gene was also confirmed by both fluorescence in situ hybridization (Figure 2*E*) and reverse transcriptase-polymerase chain reaction (Figure 2*F*). Direct sequencing of the PCR product revealed the presence of *EML4-ALK* variant 1. Thus, we referred the patient for enrollment in a clinical trial with crizotinib (PF-02341066).[2] Six weeks after administration of the crizotinib (250 mg twice a day, oral administration), the bloody sputum disappeared, and the tumor size decreased on chest computed tomography (Figure 1*C*). The carcinoembryonic antigen level also normalized. Five months after administration, an abnormal accumula-

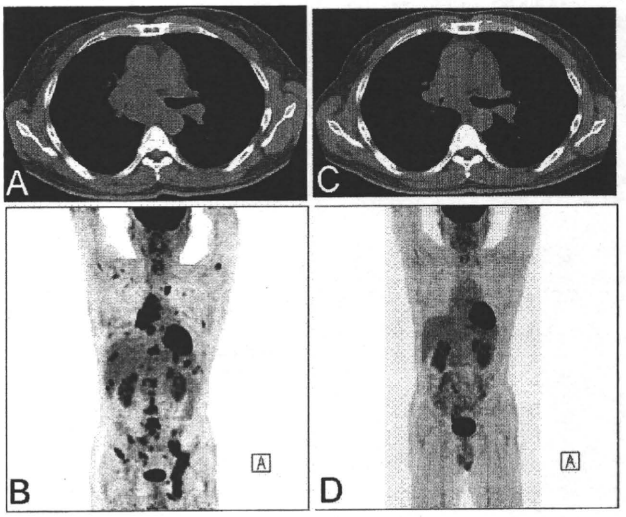

FIGURE 1. *A*, Chest computed tomography showed a narrowing of the right main bronchus due to massive lymphadenopathy. *B*, FDG-PET suggested multiple lymph node metastases and bone metastases. *C*, Six weeks after administration of the ALK inhibitor, the effect of the treatment was judged as partial response based on RECIST. *D*, Five months after administration of the ALK inhibitor, abnormal accumulation on FDG-PET had disappeared. FDG-PET, fluorodeoxyglucose positron emission tomography.

*Division of Thoracic Diseases, Chiba Cancer Center, Chiba, Japan; †Division of Thoracic Surgery, Toronto General Hospital, University Health Network, Toronto, Canada; ‡Division of Pathology, The Cancer Institute, Japanese Foundation for Cancer Research (JFCR), Koto-ku, Tokyo; and §Division of Functional Genomics, Jichi Medical University, Tochigi, Japan.

Disclosure: T.N. has received research fellowship from Uehara Memorial Foundation for the study in overseas. H.M. is a member of the scientific advisory board for Pfizer Inc. K.Y. has received unrestricted grant from Olympus Medical Corporation for Continuing Medical Education.

Address for correspondence: Takahiro Nakajima, MD, PhD, Division of Thoracic Diseases, Chiba Cancer Center, 666-2 Nitona-cho, Chuo-ku, Chiba 260-8717, Japan. E-mail: nakajii@fc.med.miyazaki-u.ac.jp

ISSN: 1556-0864/10/0512-2041

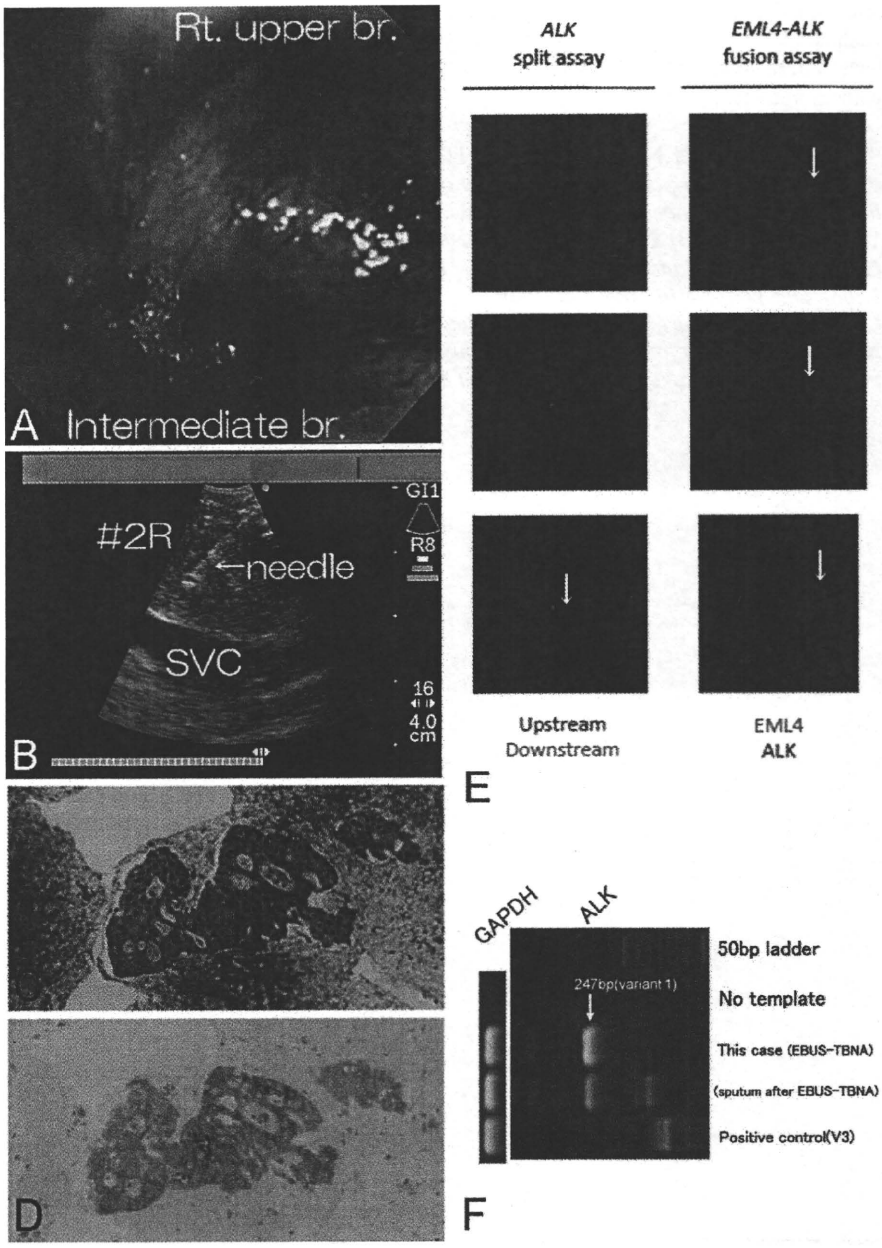

FIGURE 2. *A,* Bronchoscopic examination showed tumor compression of the right main bronchus, and the tumor had hyperplastic vessels on its surface. *B,* EBUS-TBNA was performed for a pretracheal lymph node (#2R). *C,* Histologic core revealed metastatic adenocarcinoma in #2R node. *D,* Immunohistochemistry was positive for ALK protein using the iAEP method. *E,* FISH revealed the EML4-ALK fusion gene. EML4-ALK split assay with labeled probes for the upstream (red) and downstream (green, arrow) region of the ALK locus. EML4-ALK fusion assay with labeled probes for EML4 (green, arrow) or ALK (red, arrow). Fusion gene showed EML4-ALK (arrow). *F,* RT-PCR using specific primer set for each variant also confirmed the presence of EML4-ALK variant 1 (274bp). The presence of variant 1 type fusion was also confirmed by direct sequence of the RT-PCR product (data not shown). RT-PCR, reverse transcriptase-polymerase chain reaction; FISH, fluorescence in situ hybridization.

tion almost disappeared on fluorodeoxyglucose positron emission tomography scan (Figure 1*D*). The observed side effects were only slight nausea during the early period of administration. The patient remains in good condition without tumor relapse for 10 months. The patient suddenly complained bilateral lower extremities paralysis, and the spinal cord metastasis was revealed. The patient was discontinued treatment during the trial in April 2010 because of disease progression.

DISCUSSION

Fusion of *ALK* with *EML4* gives rise to a highly potent oncogene in non-small cell lung cancer,[3] being detected in ~5% of all non-small cell lung cancer cases.[1,3,4] Presence of the ALK fusions can be detected by immunohistochemical screening[4] and can be also confirmed by fluorescence in situ hybridization and reverse transcriptase-polymerase chain reaction.[4] Recently, with progress in chemotherapeutic research, molecular targeted therapeutic agents have been developed, including ALK kinase inhibitors that are now being clinically tested.[2] Ideally, ALK fusion gene assessment should be performed using minimally invasive means to obtain biopsy samples sufficient for genetic analysis for subsequent targeted molecular therapy. Histologic as well as cytologic samples can be obtained by EBUS-TBNA, and we have previously reported that high-quality cores are adequate for molecular analyses for biomarkers.[5] The dramatic

effect of the ALK inhibitor in this patient demonstrates that adequate biomarker assessment contributes to the optimum selection of reagents in targeted molecular therapy and in individualized treatment.

ACKNOWLEDGMENTS

Supported, in part, by the Ministry of Education, Culture, Sports, Science and Technology, Grant-in-Aid for Young Scientists (B) No. 21791340 in 2009 (to T.N.), and Grant-in-Aid for Cancer Research from Ministry of Health, Labor and Welfare in 2009 (to T.N.).

The authors are grateful to Dr. Yung-Jue Bang (Seoul National University) for the treatment of this patient. They also thank Mr. Hajime Kageyama for support of molecular analysis.

REFERENCES

1. Inamura K, Takeuchi K, Togashi Y, et al. EML4-ALK lung cancers are characterized by rare other mutations, a TTF-1 cell lineage, an acinar histology, and young onset. *Mod Pathol* 2009;22:508–515.
2. Bang Y, Kwak EL, Shaw AT, et al. Clinical activity of the oral ALK inhibitor PF-02341066 in ALK-positive patients with non-small cell lung cancer (NSCLC). *J Clin Oncol* 2010;28(18s):Abstract 3.
3. Soda M, Choi YL, Enomoto M, et al. Identification of the transforming EML4-ALK fusion gene in non-small-cell lung cancer. *Nature* 2007; 448:561–566.
4. Takeuchi K, Choi YL, Togashi Y, et al. KIF5B-ALK, a novel fusion oncokinase identified by an immunohistochemistry-based diagnostic system for ALK-positive lung cancer. *Clin Cancer Res* 2009;15:3143–3149.
5. Nakajima T, Yasufuku K, Suzuki M, et al. Assessment of epidermal growth factor receptor mutation by endobronchial ultrasound-guided transbronchial needle aspiration. *Chest* 2007;132:597–602.

The American Journal of Pathology, Vol. 176, No. 3, March 2010

DOI: 10.2353/ajpath.2010.091057

Correspondence

EML4-ALK Fusion in Lung

To the Editor-in-Chief:

The recent article by Martelli and colleagues[1] reports (i) the detection of *EML4-ALK* fusion cDNA[2] not only in non-small cell lung cancer (NSCLC) specimens but in non-tumor lung tissues, (ii) a very low proportion of FISH-positive cells for *ALK* rearrangements among *EML4-ALK*–positive specimens, and (iii) the failure to detect EML4-ALK protein by immunohistochemistry (IHC) and Western blotting. Based on these lines of observation, the authors questioned the clinical relevance of *EML4-ALK* in the carcinogenesis of NSCLC.

Although detection of fusion kinases in normal tissues is a potentially interesting observation, caution is warranted in the interpretation of their results.[1,3] They replicated thrice the reverse transcription-polymerase chain reaction (RT-PCR) for *EML4-ALK* and noted that "In half of the (positive) cases, one replicate experiment did not confirm the fusion transcript was present." They then suggested that the fusion gene was "expressed at very low level." It is, however, also quite possible that such unstable PCR results may simply represent contaminated experiments. If this is the case, a discussion on FISH and protein analyses would become irrelevant. In their report, the presence of the *EML4-ALK* fusion gene was only evidenced by unstable RT-PCR results and a small proportion of FISH-positive cells among specimens.

In this regard, it was surprising that the authors had not tried genomic PCR to exclude the possibility of PCR contamination.[1,3] In most of their fusion-positive cases, they found the *EML4-ALK* variant 1 cDNA, in which exon 13 of *EML4* cDNA is connected to exon 20 of *ALK* cDNA. Because the length of intron 14 of *EML4* gene and intron 19 of *ALK* gene is 5724 bp and 1932 bp, respectively, the maximum size of the genomic PCR to detect the gene fusion should be ≈7.7 kbp, which is within the scope of current long-range PCR systems. Indeed, we have been able to detect genomic PCR products among >50% of the fusion cDNA-positive cases. Interestingly, the break/fusion points in the genome vary substantially among NSCLC specimens,[2,4,5] and we have not obtained, to date, any pairs of NSCLC specimens carrying identical break/fusion points in their genome (even among those positive for the same *EML4-ALK* variants).

We speculate, therefore, that (i) if none of the fusion cDNA-positive cases reported by Martelli et al[1,3] produce specific genomic PCR products, then the fusion cDNA products likely arose from cDNA-contamination, (ii) if the fusion cDNA–positive cases yield identical genomic PCR products, then the fusion cDNAs likely arose from specimen-contamination, and (iii) if the fusion cDNA-positive cases display distinct genomic fusion points, then each specimen was truly positive for the *EML4-ALK* fusion gene. Without such careful examination, we have to conclude that their claims in the article have not as yet been clearly demonstrated.

As described previously,[6] immunohistochemical detection of the EML4-ALK protein is highly difficult, probably owing to the weak activity of the *EML4* promoter that drives the expression of *EML4-ALK* messages. We have thus examined the suitability of commercially available antibodies to ALK for IHC and successfully developed the intercalated antibody–enhanced polymer (iAEP) method, which enables reliable detection of EML4-ALK among formalin-fixed and paraffin-embedded specimens.[6] The same specimen positive for *EML4-ALK* RT-PCR can be, for instance, readily stained to be positive with iAEP, but negative with conventional IHC methods (see Supplemental Figure S1 in ref. 6). We thus agree with Martelli et al that screening of NSCLC specimens with conventional IHC methods will not detect EML4-ALK protein, but strongly argue that such failure does not simply indicate the absence of EML4-ALK. For such screening, we recommend iAEP or other sensitive techniques.[7]

It should be further noted that, in both our[6] and other researchers' IHC analyses,[7] almost all tumor cells in a given *EML4-ALK*–positive specimen were positively immunostained with anti-ALK antibodies, suggesting a homogenous presence of *EML4-ALK* within a tumor. Such observation is, however, in contrast to the FISH data by Martelli et al, which show that the *ALK* rearrangement was only positive in ≈2% of tumor cells in a given *EML4-ALK*–positive specimen. On the contrary, FISH analyses of our *EML4-ALK*–positive samples clearly demonstrate that most of the tumor cells harbor rearranged *ALK* alleles, implying that the generation of the *EML4-ALK* fusion gene is an early event in NSCLC carcinogenesis. The homogenous presence of EML4-ALK in our fusion-positive tumors, as demonstrated by both FISH and IHC, further raises a concern about the "EML4-ALK–positive tumors" as defined by Martelli et al.

Specific inhibitors to ALK enzymatic activity are already in clinical trial, as reported at the 2009 annual meeting of America Society of Clinical Oncology and the European Cancer Organization and Congress of the European Soci-

ety for Medical Oncology.[8] Such reports reveal only modest and transient side effects (nausea, vomiting, and diarrhea) with their ALK inhibitor, but without severe damage in hematopoiesis or renal function. On the other hand, the marked therapeutic efficacy of their compound against EML4-ALK–positive NSCLC makes it one of the rare, highly successful molecular targeted therapies against human cancer, in line with imatinib mesylate and gefitinib/erlotinib. These data further reinforce the essential role of EML4-ALK in the carcinogenesis of NSCLC, and question the validity of the conclusions led by Martelli et al.[1,3]

Hiroyuki Mano
Kengo Takeuchi

Jichi Medical University, Tochigi, Japan
The University of Tokyo, Tokyo, Japan
The Cancer Institute, Tokyo, Japan

References

1. Martelli MP, Sozzi G, Hernandez L, Pettirossi V, Navarro A, Conte D, Gasparini P, Perrone F, Modena P, Pastorino U, Carbone A, Fabbri A, Sidoni A, Nakamura S, Gambacorta M, Fernandez PL, Ramirez J, Chan JK, Grigioni WF, Campo E, Pileri SA, Falini B: EML4-ALK rearrangement in non-small cell lung cancer and non-tumor lung tissues. Am J Pathol 2009, 174:661–670
2. Soda M, Choi YL, Enomoto M, Takada S, Yamashita Y, Ishikawa S, Fujiwara S, Watanabe H, Kurashina K, Hatanaka H, Bando M, Ohno S, Ishikawa Y, Aburatani H, Niki T, Sohara Y, Sugiyama Y, Mano H: Identification of the transforming *EML4-ALK* fusion gene in non-small-cell lung cancer. Nature 2007, 448:561–566
3. Sozzi G, Martelli MP, Conte D, Modena P, Pettirossi V, Pileri SA, Falini B: The EML4-ALK transcript but not the fusion protein can be expressed in reactive and neoplastic lymphoid tissues. Haematologica 2009, 94:1307–1311
4. Choi YL, Takeuchi K, Soda M, Inamura K, Togashi Y, Hatano S, Enomoto M, Hamada T, Haruta H, Watanabe H, Kurashina K, Hatanaka H, Ueno T, Takada S, Yamashita Y, Sugiyama Y, Ishikawa Y, Mano H: Identification of novel isoforms of the *EML4-ALK* transforming gene in non-small cell lung cancer. Cancer Res 2008, 68:4971–4976
5. Takeuchi K, Choi YL, Soda M, Inamura K, Togashi Y, Hatano S, Enomoto M, Takada S, Yamashita Y, Satoh Y, Okumura S, Nakagawa K, Ishikawa Y, Mano H: Multiplex reverse transcription-PCR screening for *EML4-ALK* fusion transcripts. Clin Cancer Res 2008, 14:6618–6624
6. Takeuchi K, Choi YL, Togashi Y, Soda M, Hatano S, Inamura K, Takada S, Ueno T, Yamashita Y, Satoh Y, Okumura S, Nakagawa K, Ishikawa Y, Mano H: KIF5B-ALK, a novel fusion oncokinase identified by an immunohistochemistry-based diagnostic system for ALK-positive lung cancer. Clin Cancer Res 2009, 15:3143–3149
7. Rodig SJ, Mino-Kenudson M, Dacic S, Yeap BY, Shaw A, Barletta JA, Stubbs H, Law K, Lindeman N, Mark E, Janne PA, Lynch T, Johnson BE, Iafrate AJ, Chirieac LR: Unique clinicopathologic features characterize ALK-rearranged lung adenocarcinoma in the western population. Clin Cancer Res 2009, 15:5216–5223
8. Kwak EL, Camidge DR, Clark J, Shapiro GI, Maki RG, Ratain MJ, Solomon B, Bang Y, Ou S, Salgia R: Clinical activity observed in a phase I dose escalation trial of an oral c-met and ALK inhibitor, PF-02341066. J Clin Oncol 2009, 27:15s, (suppl, abstr 3509)

Authors' reply:

In their letter, Mano and Takeuchi claim that our unstable PCR results in normal and cancerous lung tissues could be attribtuable to contamination. However, as clearly illustrated in our article,[1] serial dilution experiments in the H2228 cell line demonstrate the specificity and sensitivity of our RT-PCR assay. Furthermore, the identification in our EML4-ALK fusion positive tissues of alternative isoforms of variant 3, rather than the described two isoforms coexpressed in the H2228 cell line, is indicative of exclusive events in tumors, making contamination unlikely. Lastly, our experiments were confirmed independently in two laboratories (Milan and Barcelona) and always contained appropriate negative PCR controls.

We disagree with Mano et al's claim that the results of genomic PCR could be used to prove a possible RT-PCR contamination in our samples, which can only be excluded by the use of appropriate controls and procedures, as outlined above. However, we used genomic PCR to amplify the sequence flanking the *EML4-ALK* variant 1 breakpoint in four positive NSCLC samples. Even though a strong amplification product had been obtained from the same DNA templates using primer sets amplifying a control genomic locus of similar size to that of the cases so far reported in literature, no amplification of the *EML4-ALK* variant 1 fusion product was identified, suggesting only a minority of cells carried the *EML4-ALK* gene. These findings concur with Maes et al[2] who reported that, in lymphoid tissues, high level detection of *NPM-ALK* and *ATIC-ALK* fusion transcripts coincided with *ALK* gene rearrangements (as detected by cytogenetics and FISH), whereas low-level detection was not supported by genomic evidence of rearrangements.

In our article,[1] we clearly stated that, unlike observations in ALK+ lymphomas, tumor cells from NSCLC specimens expressed such a low amount of the EML4-ALK fusion protein that immunoprecipitation and immunohistochemistry performed with the commercially available antibodies are unable to detect it. This is in keeping with the observation that the EML4-ALK fusion protein is detectable only using highly sensitive methods, such as mass spectrometry[3] or the intercalated antibody-enhanced polymer (iAEP) method[4] which, unfortunately, are not available in all pathology laboratories and are difficult to standardize. Therefore, the question of how best to detect the EML4-ALK fusion protein remains unanswered.

Issues concerning the frequency, heterogeneity, and tissue specificity of the *EML4-ALK* rearrangement must also be addressed carefully.

Frequency

We recently extended our FISH analysis to 173 surgically resected lung cancer specimens (mainly adenocarcinoma) from an unselected group of Caucasian patients. The incidence of truly positive cases (>50% FISH positive, fusion transcript, and protein positive) was only 0.6% (1/173 cases), which reinforces the results in our artile and is in keeping with Rodig et al's[5] recent report of 1/227 (0.45%) ALK rearranged case in a series of surgically treated Western adenocarcinoma.

Heterogeneity

The heterogeneity of the *EML4-ALK* rearrangement we detected by FISH was confirmed by others in primary tumors

and cell lines[6,7] and is supported by functional studies showing that the magnitude of growth inhibition by siRNA-mediated silencing did not correlate with the number of cells harboring the rearrangement and the lack of growth inhibition in 50% of *EML4-ALK*–positive cell lines. These observations suggest that additional signaling mechanisms independent of ALK may regulate growth and cell proliferation.

Specificity

Claims from Mano's group that the *EML4-ALK* product is specific for NSCLC is contradicted by our findings in normal tissues[1,8] and by a recent study from Lin E. et al,[6] who found *EML4-ALK* fusions in breast (2.4%) and colorectal (2.4%) cancer, in addition to NSCLC.

Finally, we wonder whether it is really appropriate to compare treatments such as ALK inhibitors in NSCLC with imatinib mesylate and gefinitinib/erlotinib in other human neoplasms. In fact: i) the role of EML4-ALK in NSCLC is not as well established as that of BCR/ABL in chronic myeloid leukemia (CML); ii) NSCLC responses to ALK inhibitors[9] are not as remarkable as the CML response to imatinib mesylate; and iii) patients with NSCLC were treated with a multikinase, c-MET and ALK, inhibitor.[9] Considering that about 20% of NSCLC have MET amplification and overexpression and that MET rearrangements are homogeneous in lung cancer,[10] it may be possible that responses to the multikinase inhibitor may be related to other coexisting oncogenic events, independently of ALK.

In conclusion, although we fully acknowledge the importance of Soda et al's discovery,[11] we believe that additional studies are required to elucidate the concurrent genetic events and cellular settings necessary for *EML4-ALK* to exert an oncogenic function and to better define the role of *EML4-ALK* in diagnosis and targeted therapy of NSCLC.

Brunangelo Falini
Maria Paola Martelli
Stefano A. Pileri
Gabriella Sozzi
Patrizia Gasparini

Institute of Hematology, University of Perugia, Perugia, Italy
The Units of Surgical Pathology and Hematopathology,
S. Orsola Hospital, University of Bologna, Bologna, Italy
Fondazione IRCCS, Istituto Nazionale dei Tumori, Milan, Italy

References

1. Martelli MP, Sozzi G, Hernandez L, Pettirossi V, Navarro A, Conte D, Gasparini P, Perrone F, Modena P, Pastorino U, Carbone A, Fabbri A, Sidoni A, Nakamura S, Gambacorta M, Fernandez PL, Ramirez J, Chan JK, Grigioni WF, Campo E, Pileri SA, Falini B: EML4-ALK rearrangement in non-small cell lung cancer and non-tumor lung tissues. Am J Pathol 2009, 174:661–670
2. Maes B, Vanhentenrijk V, Wlodarska I, Cools J, Peeters B, Marynen P, de Wolf-Peeters C: The NPM-ALK and the ATIC-ALK fusion genes can be detected in non-neoplastic cells. Am J Pathol 2001, 158: 2185–2193
3. Rikova K, Guo A, Zeng Q, Possemato A, Yu J, Haack H, Nardone J, Lee K, Reeves C, Li Y, Hu Y, Tan Z, Stokes M, Sullivan L, Mitchell J, Wetzel R, Macneill J, Ren JM, Yuan J, Bakalarski CE, Villen J, Kornhauser JM, Smith B, Li D, Zhou X, Gygi SP, Gu TL, Polakiewicz RD, Rush J, Comb MJ: Global survey of phosphotyrosine signaling identifies oncogenic kinases in lung cancer. Cell 2007, 131:1190–1203
4. Takeuchi K, Choi YL, Togashi Y, Soda M, Hatano S, Inamura K, Takada S, Ueno T, Yamashita Y, Satoh Y, Okumura S, Nakagawa K, Ishikawa Y, Mano H: KIF5B-ALK, a novel fusion oncokinase identified by an immunohistochemistry-based diagnostic system for ALK-positive lung cancer. Clin Cancer Res 2009, 15:3143–3149
5. Rodig SJ, Mino-Kenudson M, Dacic S, Yeap BY, Shaw A, Barletta JA, Stubbs H, Law K, Lindeman N, Mark E, Janne PA, Lynch T, Johnson BE, Iafrate AJ, Chirieac LR: Unique clinicopathologic features characterize ALK-rearranged lung adenocarcinoma in the western population. Clin Cancer Res 2009, 15:5216–5223
6. Lin E, Li L, Guan Y, Soriano R, Rivers CS, Mohan S, Pandita A, Tang J, Modrusan Z: Exon array profiling detects EML4-ALK fusion in breast, colorectal, and non-small cell lung cancers. Mol Cancer Res 2009, 7:1466–1476
7. Perner S, Wagner PL, Demichelis F, Mehra R, Lafargue CJ, Moss BJ, Arbogast S, Soltermann A, Weder W, Giordano TJ, Beer DG, Rickman DS, Chinnaiyan AM, Moch H, Rubin MA: EML4-ALK fusion lung cancer: a rare acquired event. Neoplasia 2008, 10:298–302
8. Sozzi G, Martelli MP, Conte D, Modena P, Pettirossi V, Pileri SA, Falini B: The EML4-ALK transcript but not the fusion protein can be expressed in reactive and neoplastic lymphoid tissues. Haematologica 2009, 94:1307–1311
9. Kwak E, Camidge D, Clark J, Shapiro G, Maki R, Ratain M, Solomon B, Bang Y, Ou S, Salgia R: Clinical acitvity observed in a phase I dose escalation trial of an oral c-met and ALK inhibitor, PF-02341066. J Clin Oncol 2009, 27:15s (Suppl, Abstr 3509)
10. Beau-Faller M, Ruppert AM, Voegeli AC, Neuville A, Meyer N, Guerin E, Legrain M, Mennecier B, Wihlm JM, Massard G, Quoix E, Oudet P, Gaub MP: MET gene copy number in non-small cell lung cancer: molecular analysis in a targeted tyrosine kinase inhibitor naive cohort. J Thorac Oncol 2008, 3:331–339
11. Soda M, Choi YL, Enomoto M, Takada S, Yamashita Y, Ishikawa S, Fujiwara S, Watanabe H, Kurashina K, Hatanaka H, Bando M, Ohno S, Ishikawa Y, Aburatani H, Niki T, Sohara Y, Sugiyama Y, Mano H: Identification of the transforming EML4-ALK fusion gene in non-small-cell lung cancer. Nature 2007, 448:561–566

Cancer Science
The official journal of the Japanese Cancer Association

Identification of transforming activity of free fatty acid receptor 2 by retroviral expression screening

Hisashi Hatanaka,[1,2] Mamiko Tsukui,[2] Shuji Takada,[1] Kentaro Kurashina,[1,3] Young Lim Choi,[1,4] Manabu Soda,[1] Yoshihiro Yamashita,[1] Hidenori Haruta,[1,3] Toru Hamada,[1,3] Toshihide Ueno,[1] Kiichi Tamada,[2] Yoshinori Hosoya,[3] Naohiro Sata,[3] Yoshikazu Yasuda,[3] Hideo Nagai,[3] Kentaro Sugano[2] and Hiroyuki Mano[1,4,5,6]

Divisions of [1]Functional Genomics, [2]Gastroenterology, [3]Department of Surgery, Jichi Medical University, Tochigi; [4]Department of Medical Genomics, Graduate School of Medicine, The University of Tokyo, Tokyo; [5]CREST, Japan Science and Technology Agency, Saitama, Japan

(Received May 4, 2009/Revised August 22, 2009/Accepted August 30, 2009/Online publication September 24, 2009)

Gallbladder cancer (GBC) is a highly fatal malignancy in humans. Genetic alterations in *KRAS* or *TP53* as well as overexpression of *ERBB2* have been shown to contribute to the development of certain types of GBC. However, many cases of GBC do not harbor such genetic changes, with other transforming events awaiting discovery. We here tried to identify novel cancer-promoting genes in GBC, with the use of a retroviral cDNA expression library. A retroviral cDNA expression library was constructed from a surgically resected clinical specimen of GBC, and was used to infect 3T3 fibroblasts in a focus formation assay. cDNA incorporated into the transformed foci was rescued by PCR. One such cDNA was found to encode free fatty acid receptor 2 (FFAR2), a G protein-coupled receptor for short-chain fatty acids. The oncogenic potential of *FFAR2* was confirmed both *in vitro* with the focus formation assay and by evaluation of cell growth in soft agar as well as *in vivo* with a tumorigenicity assay in nude mice. The isolated *FFAR2* cDNA had no sequence alterations, suggesting that upregulation of *FFAR2* expression may contribute to malignant transformation. Indeed, all of quantitative RT-PCR, *in situ* hybridization, and immunohistochemical analyses showed that the amount of *FFAR2* mRNA and its protein product was increased in digestive tract cancer specimens. Furthermore, short-chain fatty acids potentiated the mitogenic action of FFAR2 in 3T3 cells. Our data thus, for the first time, implicate FFAR2 in carcinogenesis of the digestive tract. (*Cancer Sci* 2010; 101: 54–59)

Gallbladder cancer (GBC) is a highly fatal malignancy in humans, being most prevalent in South America and Asia. In most cases, GBC is not diagnosed until it has reached an advanced stage, when the 5-year survival rate is ~10%.[1,2] In the USA, ~8000 new cases of biliary tract cancer (BTC) are diagnosed each year, with ~4000 of the affected individuals subsequently dying of GBC.[3] Several risk factors have been identified for GBC, including cholelithiasis[4] and anomalous pancreaticobiliary duct junction.[5] Genetic alterations in *KRAS* or *TP53* as well as overexpression of *ERBB2* have been shown to contribute to the development of certain types of GBC. However, many cases of GBC do not harbor such genetic changes, with other transforming events awaiting discovery.

The focus formation assay with 3T3 or RAT1 fibroblasts has been used extensively to screen for transforming genes in various carcinomas.[6] In such screening, genomic DNA is isolated from cancer specimens and used to transfect fibroblasts, potentially resulting in the development of transformed cell foci. However, given that expression of the introduced genes is controlled by their own promoters or enhancers, oncogenes in cancer cells may exert effects in fibroblasts only when their control regions are active in these cells, which is not guaranteed.

Adequate expression of cDNA in fibroblasts can be achieved by placing them under the control of an exogenous promoter fragment. Toward this goal, we have recently established a retroviral cDNA expression library system that is sensitive enough to generate libraries with a high complexity even from small amounts of materials such as clinical specimens.[7–9] With this system, we have successfully discovered a fusion-type protein tyrosine kinase EML4–ALK in non-small cell lung cancer.[7]

In this manuscript, we have applied this technology to a surgically resected clinical specimen of GBC, and used this library to screen for transforming genes in GBC. Unexpectedly, transforming ability has been discovered for free fatty acid receptor 2 (FFAR2, also known as GPR43), which functions as a cellular receptor for short-chain fatty acids (SCFA).[10] Further, tumor-specific expression of FFAR2 has been proven among a panel of clinical specimens for GBC, gastric cancer, and colorectal cancer (CRC) by *in situ* hybridization and immunohistochemical analyses, indicating tumor-promoting activity among digestive tract cancers.

Materials and Methods

Clinical specimens and cells lines. Resected clinical materials were obtained from individuals who underwent surgery at Jichi Medical University Hospital. Written informed consent was obtained from each subject according to the protocols approved by the ethics committees of Jichi Medical University. Mouse 3T3 and BOSC23 cell lines were obtained from American Type Culture Collection (Manassas, VA, USA), and maintained in Dulbecco's modified Eagle medium/F12 (DMEM/F12; Invitrogen, Carlsbad, CA, USA) containing 10% fetal bovine serum (Invitrogen) and 2 mM L-glutamine.

Construction of retroviral cDNA expression library. The retroviral cDNA library was constructed as described previously.[7–9,11] Briefly, first-strand cDNA was synthesized from the RNA with the use of PowerScript reverse transcriptase, the SMART IIA oligonucleotide, and CDS primer IIA (all from Clontech, Mountain View, CA, USA). The resulting cDNA was then amplified by PCR with 5′-PCR primer IIA (Clontech) and PrimeSTAR HS DNA polymerase (Takara Bio, Otsu, Shiga, Japan) for 17 cycles of 98°C for 10 s and 68°C for 6 min. The PCR products were ligated to a BstXI adapter (Invitrogen) and then incorporated into the pMXS retroviral plasmid (kindly provided by T. Kitamura of the Institute of Medical Science, University of Tokyo).

Recombinant retroviruses were produced by introduction of the plasmid library into the packaging cell line BOSC23[12] and were used to infect 3T3 cells in the presence of polybrene (4 μg/mL; Sigma, St Louis, MO, USA). The cells were cultured for 2 weeks, after which transformed foci were isolated, expanded, and subjected to extraction of genomic DNA. Insert

[6]To whom correspondence should be addressed. E-mail: hmano@jichi.ac.jp

doi: 10.1111/j.1349-7006.2009.01348.x

cDNA was recovered from the genomic DNA by PCR with 5′-PCR primer IIA and PrimeSTAR HS DNA polymerase. Amplified products were then ligated to the plasmid pT7Blue-2 (Novagen, Madison, WI, USA) and subjected to nucleotide sequencing.

Transformation assay. For a focus formation assay, recombinant retrovirus was used to infect 3T3 cells for 48 h. The culture medium of 3T3 cells was then changed to DMEM/F12 supplemented with 5% calf serum and 2 mM L-glutamine, and incubated for 2 weeks. To examine anchorage-independent growth in soft agar, 3T3 cells infected with retrovirus were resuspended in culture medium containing 0.4% agar (SeaPlaque GTG agarose; Cambrex, East Rutherford, NJ, USA), and seeded onto a base layer of complete medium containing 0.5% agar. Cell growth was assessed after 3 weeks of incubation.

For an *in vivo* tumorigenicity assay, 3T3 cells (2×10^6) infected with the retrovirus expressing FFAR2 were resuspended in 500 μL PBS, and injected into each shoulder of *nu/nu* BALB/c mice (6 weeks old). Tumor formation was assessed after 3 weeks.

Quantitation with real-time RT-PCR. Oligo(dT)-primed cDNA was synthesized from the clinical specimens with PowerScript reverse transcriptase, and subjected to quantitative PCR with a QuantiTect SYBR Green PCR kit (Qiagen, Valencia, CA, USA) and an amplification protocol consisting of incubations at 94°C for 15 s, 60°C for 30 s, and 72°C for 60 s. Incorporation of the SYBR Green dye into PCR products was monitored in real time with an ABI PRISM 7900HT sequence detection system (Applied Biosystems, Foster City, CA, USA), thereby allowing determination of the threshold cycle (C_T) at which exponential amplification of products begins. The C_T values for cDNA corresponding to the β-actin gene (*ACTB*) and *FFAR2* were used to calculate the abundance of the latter mRNA relative to that of the former. The oligonucleotide primers used for PCR were 5′-CCATCATGAAGTGTGACGTGG-3′ and 5′-GTCCGCCTAGAAGCATTTGCG-3′ for *ACTB* and 5′-CACTCAACGCCAGTCTGGAC-3′ and 5′-TGGCATCCCTTCTCCTTGAC-3′ for *FFAR2*.

In situ hybridization with sense or antisense riboprobes corresponding to the 3′ region (nucleotides 867–1229) of the *FFAR2* cDNA isolated in this study was conducted as described previously.[13]

Immunohistochemistry. Human tissues were fixed in 4% formaldehyde in PBS at room temperature overnight, embedded in paraffin, and sectioned at a thickness of 3 μm. Sections were mounted on glass slides, deparaffinized through three changes of xylene for 4 min each, and rehydrated in distilled water through a series of graded alcohols. For histological evaluation, sections were stained with hematoxylin–eosin solutions. For immunohistochemical experiments, antigenicity was enhanced by boiling the sections in 10 mM citrate buffer (pH 6.0) in a microwave oven for 15 min, and the endogenous peroxidase activity was blocked by incubation in methanol containing 0.3% H_2O_2 for 30 min. After two washes with PBS containing 1% Triton X-100, the sections were preincubated with the blocking buffer (#X0909; Dako, Glostrup, Denmark) in a humidified chamber for 20 min at room temperature, and then incubated with anti-FFAR2 antibody (SP4226P; Acris Antibodies, Schillerstaβe, Herford, Germany) at 4°C overnight. Next, the sections were washed in PBS and incubated with horseradish peroxidase (HRP)-labeled polymers conjugated to goat antirabbit immunoglobulin (#K4003; Dako) at 37°C for 30 min. Color development was carried out by incubating the sections with 3,3-diaminobenzidine tetrahydrochloride (Wako Pure Chemical Industries, Osaka, Japan) as a chromogenic substrate. Finally, the sections were lightly counterstained with hematoxylin, mounted, and viewed under a light microscope.

Cell proliferation assay. Mouse 3T3 cells expressing FFAR2 or not expressing FFAR2 were seeded into 96-well plates at a concentration of 4×10^3 cells/well, and incubated for 24 h with DMEM-F12 medium and 1% charcoal-treated fetal bovine serum (Invitrogen). Cells were further cultured for 48 h with 100 mM sodium acetate or 1 mM sodium butyrate, and were subjected to the cell proliferation assay with the WST-1 reagent (Clontech).

Results

Focus formation assay with a GBC library. To screen for transforming genes in digestive tract cancers, we constructed a retroviral cDNA expression library from a surgically resected GBC specimen, and obtained a total of 3.2×10^5 colony-forming units of independent plasmid clones, from which we randomly selected 20 clones and examined the incorporated cDNA. An insert of ≥500 bp was present in 16 (80%) of the plasmid clones, and the average size of these inserts was 1.48 kbp (data not shown). Infection of mouse NIH 3T3 fibroblasts with the recombinant retroviral library generated a total of 89 transformed foci (Fig. 1a). No foci were obtained for cells infected with the empty virus, whereas numerous foci were readily apparent for cells infected with a virus encoding the v-Ras oncoprotein.

Each focus obtained with the cDNA expression library was isolated, expanded independently, and used to prepare genomic DNA for recovery of retroviral inserts by PCR with the primers used originally to amplify the cDNA in construction of the library.[7] We recovered a total of 45 cDNA fragments by PCR, each of which was subjected to nucleotide sequencing in both directions. Screening of the 45 cDNA sequences against the public nucleotide sequence databases revealed that they corresponded to 19 independent genes (Supporting Information Table S1). To confirm the transforming potential of the isolated cDNA, we ligated each cDNA clone to pMXS and used the resulting retroviruses to infect 3T3 cells. The focus formation assay was carried out for cDNA corresponding to 19 independent genes, revealing reproducible transforming activity for: clone ID #2, corresponding to *ARHGEF1* (GenBank accession number NM_004706); clone ID #6, corresponding to *TBC1D3* (GenBank accession number NM_032258); clone ID #7, corresponding to *FGF4* (GenBank accession number NM_002007); and clone ID #14, corresponding to *FFAR2* (GenBank accession number NM_005306) (Fig. 1b).

FFAR2 as an oncogene. FFAR2 functions as a cellular receptor for SCFA,[10] and is expressed in the digestive tract.[14] It is thought to respond to fatty acids released in the digestive tract, but has not previously been shown to possess transforming potential. We therefore focused on FFAR2 in our subsequent analyses. Given that nucleotide sequencing of clone ID #14 did not reveal any sequence alterations compared to the published cDNA sequence of *FFAR2* (GenBank accession number NM_005306), we hypothesized that overexpression of *FFAR2* might contribute to malignant transformation.

We then assessed the transforming activity of FFAR2 in 3T3 cells with a soft-agar assay. Whereas cells infected with the empty virus did not grow in soft agar, those infected with a virus encoding v-Ras grew readily (Fig. 1b). Cells infected with a virus encoding FFAR2 also formed multiple foci in repeated experiments, indicative of the ability of FFAR2 to confer the property of anchorage-independent growth on 3T3 cells. We further tested the activity of FFAR2 in an *in vivo* tumorigenicity assay with athymic nude mice. 3T3 cells infected with the empty virus or with retroviruses encoding FFAR2 or v-Ras were thus injected subcutaneously into the mice. Tumor formation was readily apparent for the cells expressing FFAR2 or v-Ras (Fig. 1b).

Overexpression of FFAR2 in digestive tract cancers. Given that our data revealed an unexpected transforming potential of FFAR2 (at least, when it is abundantly expressed), we examined

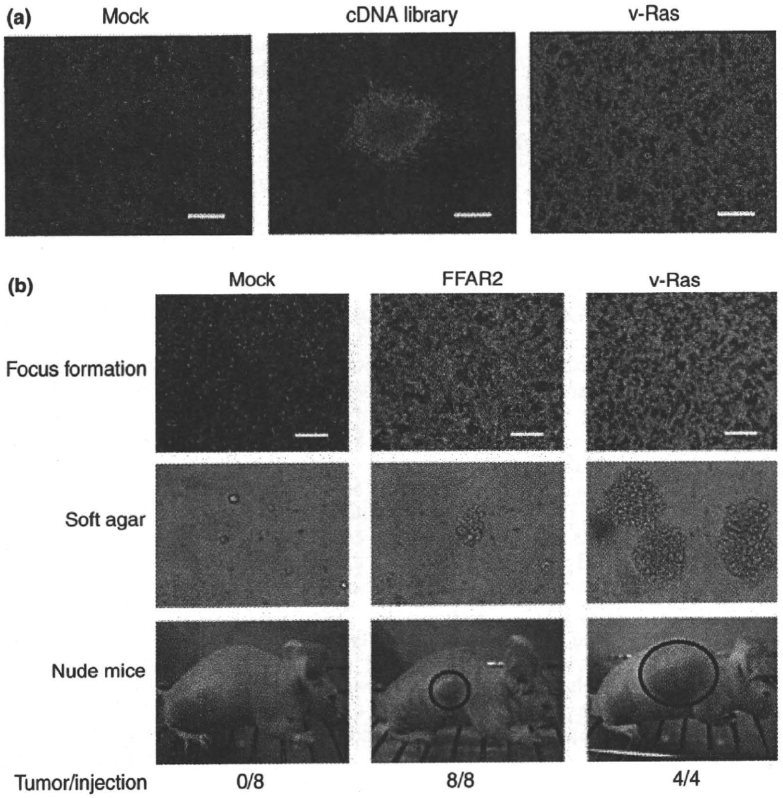

Fig. 1. Transforming activity of free fatty acid receptor 2 (FFAR2). (a) A retroviral cDNA expression library was constructed from a gallbladder cancer specimen isolated from a 64-year-old man. Mouse 3T3 cells were infected with the retroviral cDNA library, a virus encoding v-Ras, or the empty virus (Mock), and were photographed after culture for 2 weeks for the analysis of focus formation. Scale bars = 1 mm. (b) 3T3 cells were infected with viruses encoding FFAR2 or v-Ras or with the empty virus (Mock) and were then cultured for 5 days for analysis of focus formation (top panels: scale bars = 1 mm). The same batches of 3T3 cells were also assayed for anchorage-independent growth in soft agar over 17 days (middle panels) and for tumorigenicity in nude mice over 3 weeks (bottom panels). Tumors formed in the shoulders of mice injected subcutaneously with 1×10^5 cells are indicated by red circles. The frequency of tumor formation (tumor/injection) is also indicated.

whether FFAR2 might be overexpressed in human cancer specimens. We prepared oligo(dT)-primed cDNA from seven specimens of BTC, 89 specimens of gastric cancer, and 80 specimens of CRC by reverse transcription and then subjected the cDNA preparations to quantitative PCR analysis in order to measure the amount of *FFAR2* cDNA. For comparison, we also analyzed specimens of normal gallbladder ($n = 6$) and biliary duct ($n = 1$) as well as paired noncancerous tissue for all specimens of gastric cancer and CRC. Whereas the mean expression level of *FFAR2* seemed higher in BTC compared to normal gallbladder/biliary duct, a large standard deviation in the expression level made the difference insignificant ($P > 0.05$) (Fig. 2a). However, the *FFAR2* level was significantly increased ($P < 0.05$) in gastric cancer (Fig. 2b) and CRC (Fig. 2c) compared with the corresponding paired normal tissue specimens.

To examine further the site and extent of *FFAR2* expression, we carried out *in situ* hybridization analysis with a series of cancer specimens. First, a section of a CRC specimen was subjected to hybridization with sense or antisense probe for *FFAR2* mRNA. Only the antisense probe yielded clear signals in the cytoplasm and nucleus of the cancer cells (Fig. 3a), thus confirming the specificity of this probe. A series of cancer specimens was then subjected to hybridization with the antisense probe for *FFAR2* mRNA. GBC cells exhibited an increased level of hybridization compared with the normal cells in the same section (Fig. 3b). However, epithelial cells of normal gall-

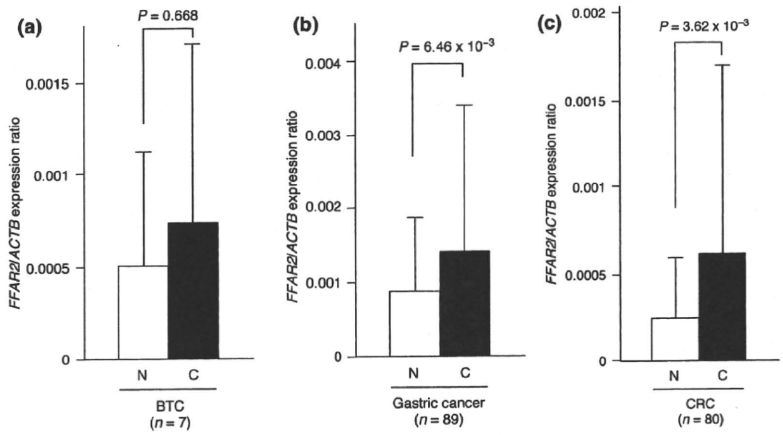

Fig. 2. Expression of free fatty acid receptor 2 (*FFAR2*) in digestive tract cancers. Oligo(dT)-primed cDNA was synthesized from (a) clinical specimens of biliary tract cancer (C) or normal gallbladder and biliary tract tissue (N), or from paired cancerous (C) and noncancerous (N) tissue specimens from patients with (b) gastric cancer or (c) colorectal cancer. The resultant cDNA was subjected to quantitative PCR analysis. Data are means + SD for the indicated *n* values, and *P*-values for the indicated comparisons were determined by Student's *t*-test. ACTB, β-actin.

doi: 10.1111/j.1349-7006.2009.01348.x

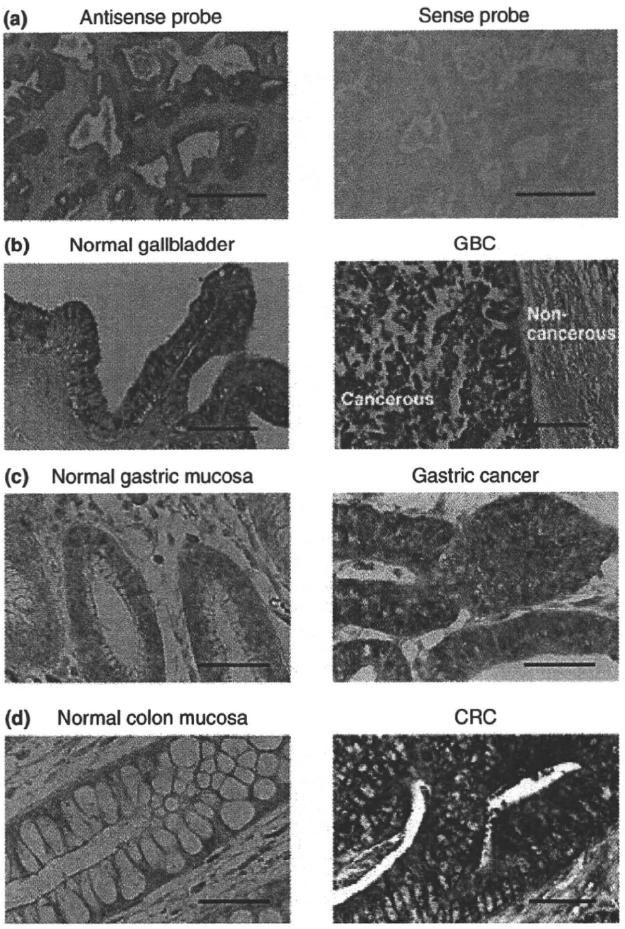

Fig. 3. *In situ* hybridization analysis of free fatty acid receptor 2 (*FFAR2*) expression. (a) A section of colorectal cancer (CRC) was subjected to *in situ* hybridization with sense or antisense riboprobes corresponding to the 3′ region (nucleotides 867–1229) of the *FFAR2* cDNA isolated in this study. (b–d) Sections of (b) normal gallbladder and gallbladder cancer (GBC), (c) paired normal gastric mucosa and gastric cancer, and (d) paired normal colon mucosa and CRC were also subjected to *in situ* hybridization with the antisense probe for *FFAR2* mRNA. Scale bars = 1 mm (a), 100 μm (b), or 50 μm (c,d).

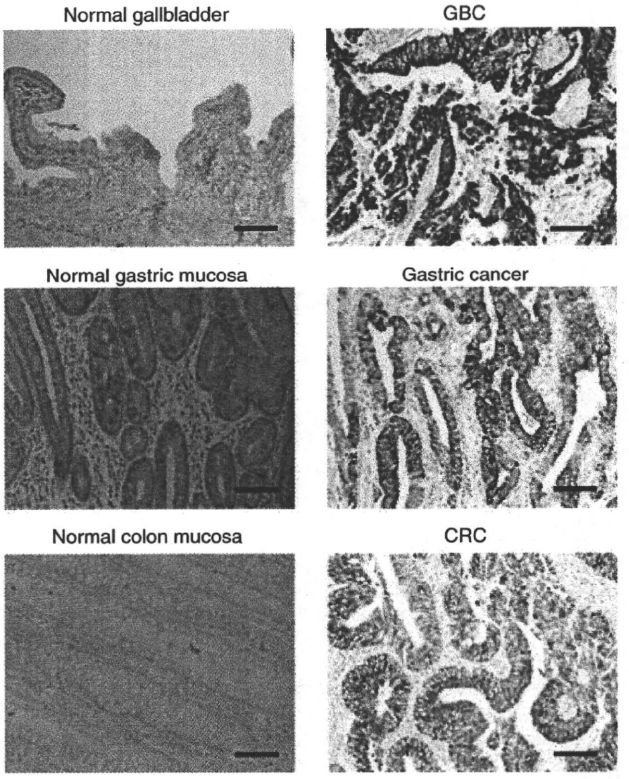

Fig. 4. Immunohistochemical analysis of free fatty acid receptor 2 (FFAR2) expression. Sections of normal gallbladder and gallbladder cancer (GBC) (upper panel), of paired normal gastric mucosa and gastric cancer (middle panel), and of paired normal colon mucosa and colorectal cancer (CRC) (lower panel) were subjected to immunohistochemical staining with antibody to FFAR2. Scale bars = 100 μm.

bladder were also stained with the probe, possibly explaining why the amount of *FFAR2* mRNA did not differ significantly between GBC and normal tissue by quantitative RT-PCR analysis (Fig. 2a). In contrast, the hybridization signal for *FFAR2* mRNA was markedly greater both in gastric cancer cells in eight of 10 specimens examined than in gland cells of the normal stomach (Fig. 3c), as well as in CRC cells in 13 of 14 specimens examined compared with the corresponding normal cells (Fig. 3d), consistent with the data obtained by quantitative RT-PCR analysis (Fig. 2b,c).

Additionally, we further examined the FFAR2 protein level by immunohistochemistry with anti-FFAR2 antibody among digestive tract cancers. As shown in Figure 4, FFAR2 was apparently induced in a GBC specimen (from which the cDNA library was generated) compared to normal gallbladder, in a gastric cancer specimen compared to its paired normal mucosa, and in a CRC specimen compared to the paired normal mucosa.

Ligand-mediated mitogenic signals of FFAR2. Given that SCFA are the presumptive ligands for FFAR2, we next examined whether the transforming activity of FFAR2 might be stimulated by its binding of such ligands. Toward this end, we incubated 3T3 cells expressing *FFAR2* cDNA in the absence or presence of the SCFA sodium acetate or sodium butyrate. Forced expression of FFAR2 induced a small increase in the growth rate of 3T3 cells even in the absence of the SCFA, whereas the SCFA had no effect on the growth of cells not expressing FFAR2. In contrast, sodium acetate (100 mM) induced a pronounced increase in the growth rate of cells expressing FFAR2 (Fig. 5a). A smaller but still significant increase in the growth rate of cells expressing FFAR2 was also induced by the addition of 1 mM sodium butyrate (Fig. 5b).

Discussion

In this study, we constructed a retroviral cDNA expression library for a GBC specimen and thereby identified the transforming potential of FFAR2. In response to its activation by ligand, FFAR2 regulates lipogenesis,[14] neutrophil migration,[15] and intestinal motility.[16] Although SCFA activate the p38 mitogen-activated protein kinase and heat shock protein 27 signaling pathway via FFAR2 in MCF-7 human breast cancer cells,[17] a relationship between FFAR2 and carcinogenesis has not previously been described.

The *FFAR2* gene has been shown to be preferentially expressed in stomach, small intestine, colon, spleen, and adipose tissue of mice.[14] A substantial amount of *FFAR2* mRNA was also detected in the rat gut, with the highest levels apparent in the colon and lower levels observed in esophagus and stom-

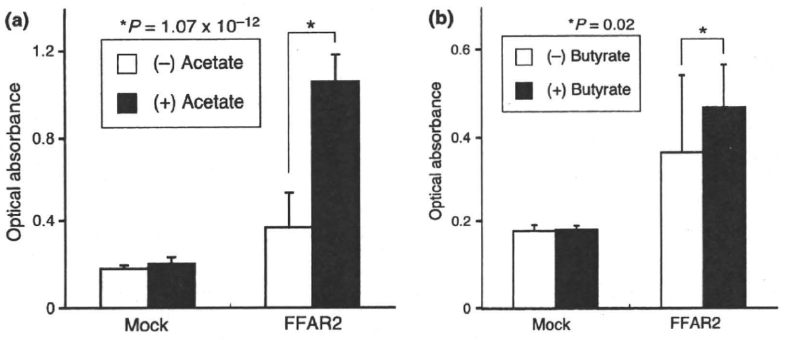

Fig. 5. Effect of short chain fatty acids on the proliferation of cells expressing free fatty acid receptor 2 (FFAR2). Mouse 3T3 cells infected with a virus encoding FFAR2 or with the empty virus (Mock) were cultured for 48 h in DMEM-F12 medium supplemented with 1% charcoal-treated fetal bovine serum in the absence or presence of (a) 100 mM sodium acetate or (b) 1 mM sodium butyrate. Cell proliferation was then assayed with the use of the WST-1 reagent. Data are expressed as absorbance at 450 nm and are means + SD of values from three independent experiments. *P*-values for the indicated comparisons were determined by Student's *t*-test.

ach.[16] In addition, FFAR2 has been detected in enterocytes of the rat intestine[18] as well as in those of the human colon.[19] The preferential expression of FFAR2 in the digestive tract and the mitogenic activity of the encoded protein together suggest a possible role for FFAR2 in carcinogenesis of the digestive system.

In our current analyses, both mRNA and protein amounts for *FFAR2* were frequently induced among the specimens for digestive tract cancer. However, DNA quantitation of the *FFAR2* locus failed to detect copy number changes of the genome (data not shown), and there are no CpG islands mapped closely or within the *FFAR2* locus in the human genome. Therefore, the molecular mechanism underlying such *FFAR2* induction is yet to be revealed.

SCFA, such as acetate, propionate, and butyrate, are the major products of the breakdown of dietary fiber by bacterial fermentation in the mammalian small and large intestine.[20] Among various SCFA, acetate has the highest selectivity for FFAR2.[21] The composition of SCFA in the colonic lumen is ~60% acetate, ~20% propionate, and ~20% butyrate.[22] SCFA are the major anions, being present at a total concentration of ~100 mM, in the lumen of the large intestine in mammals.[23] We found that the mitogenic effect of acetate in 3T3 cells expressing FFAR2 was maximal at ~100 mM (data not shown). These data suggest that FFAR2 may induce mitogenesis in the digestive tract in a manner dependent on the content of SCFA (especially that of acetate) in the diet.

It should be noted that a mere overexpression of FFAR2 significantly induced the growth of 3T3 cells even without the SCFA stimulation (Fig. 5). Although this observation potentially indicates a novel, SCFA-independent function of FFAR2, overexpression of cell surface receptors often stimulates their intracellular signaling with suboptimal concentrations of cognate ligands. Therefore, it is also possible that highly abundant FFAR2 proteins have evoked a mitogenic signaling in 3T3 in response to a low level of SCFA in the serum (or even independent of SCFA).

Diet has a substantial impact on the occurrence of digestive tract cancers, including GBC, gastric cancer, and CRC,[24] as well as on that of chronic inflammatory bowel diseases.[25] Our present findings suggest a possible connection between such disorders and either continuous exposure to SCFA in certain types of diet or induced expression of FFAR2 in the digestive tract. FFAR2 is thus a potential therapeutic target for these disorders.

Acknowledgments

We thank K. Sasaki for technical assistance and T. Kitamura (Institute of Medical Science, University of Tokyo) for the pMXS retroviral plasmid. This study was supported in part by Grants-in-Aid for Scientific Research from the Ministry of Education, Culture, Sports, Science, and Technology, Japan, and by grants from the Japan Society for the Promotion of Science, and from the Ministry of Health, Labour, and Welfare, Japan. The nucleotide sequence of the *FFAR2* cDNA isolated in this study has been deposited in DDBJ/GenBank under the accession number AB378083.

Abbreviations

ALK	anaplastic lymphoma kinase
EML4	echinoderm microtubule associated protein like-4
ERBB2	v-erb-b2 avian erythroblastic leukemia viral oncogene homolog 2
KRAS	v-ki-ras2 Kirsten rat sarcoma viral oncogene homolog
TP53	tumor protein p53

References

1 Carriaga MT, Henson DE. Liver, gallbladder, extrahepatic bile ducts, and pancreas. *Cancer* 1995; **75**: 171–90.
2 Cubertafond P, Gainant A, Cucchiaro G. Surgical treatment of 724 carcinomas of the gallbladder. Results of the French Surgical Association Survey. *Ann Surg* 1994; **219**: 275–80.
3 Jemal A, Siegel R, Ward E, Murray T, Xu J, Thun MJ. Cancer statistics, 2007. *CA Cancer J Clin* 2007; **57**: 43–66.
4 Zatonski WA, Lowenfels AB, Boyle P *et al.* Epidemiologic aspects of gallbladder cancer: a case–control study of the SEARCH Program of the International Agency for Research on Cancer. *J Natl Cancer Inst* 1997; **89**: 1132–8.
5 Hasumi A, Matsui H, Sugioka A *et al.* Precancerous conditions of biliary tract cancer in patients with pancreaticobiliary maljunction: reappraisal of nationwide survey in Japan. *J Hepatobiliary Pancreat Surg* 2000; **7**: 551–5.
6 Goldfarb M, Shimizu K, Perucho M, Wigler M. Isolation and preliminary characterization of a human transforming gene from T24 bladder carcinoma cells. *Nature* 1982; **296**: 404–9.
7 Soda M, Choi YL, Enomoto M *et al.* Identification of the transforming *EML4–ALK* fusion gene in non-small-cell lung cancer. *Nature* 2007; **448**: 561–6.
8 Hatanaka H, Takada S, Choi YL *et al.* Transforming activity of purinergic receptor P2Y, G-protein coupled, 2 revealed by retroviral expression screening. *Biochem Biophys Res Commun* 2007; **356**: 723–6.
9 Choi YL, Kaneda R, Wada T *et al.* Identification of a constitutively active mutant of JAK3 by retroviral expression screening. *Leuk Res* 2007; **31**: 203–9.
10 Brown AJ, Goldsworthy SM, Barnes AA *et al.* The Orphan G protein-coupled receptors GPR41 and GPR43 are activated by propionate and other short chain carboxylic acids. *J Biol Chem* 2003; **278**: 11312–9.
11 Fujiwara S, Yamashita Y, Choi YL *et al.* Transforming activity of purinergic receptor P2Y, G protein coupled, 8 revealed by retroviral expression screening. *Leuk Lymphoma* 2007; **48**: 978–86.
12 Pear WS, Nolan GP, Scott ML, Baltimore D. Production of high-titer helper-free retroviruses by transient transfection. *Proc Natl Acad Sci USA* 1993; **90**: 8392–6.
13 Schaeren-Wiemers N, Gerfin-Moser A. A single protocol to detect transcripts of various types and expression levels in neural tissue and cultured cells: in

doi: 10.1111/j.1349-7006.2009.01348.x

situ hybridization using digoxigenin-labelled cRNA probes. *Histochemistry* 1993; **100**: 431–40.
14 Hong YH, Nishimura Y, Hishikawa D *et al.* Acetate and propionate short chain fatty acids stimulate adipogenesis via GPCR43. *Endocrinology* 2005; **146**: 5092–9.
15 Nilsson NE, Kotarsky K, Owman C, Olde B. Identification of a free fatty acid receptor, FFA2R, expressed on leukocytes and activated by short-chain fatty acids. *Biochem Biophys Res Commun* 2003; **303**: 1047–52.
16 Dass NB, John AK, Bassil AK *et al.* The relationship between the effects of short-chain fatty acids on intestinal motility in vitro and GPR43 receptor activation. *Neurogastroenterol Motil* 2007; **19**: 66–74.
17 Yonezawa T, Kobayashi Y, Obara Y. Short-chain fatty acids induce acute phosphorylation of the p38 mitogen-activated protein kinase/heat shock protein 27 pathway via GPR43 in the MCF-7 human breast cancer cell line. *Cell Signal* 2007; **19**: 185–93.
18 Karaki S, Mitsui R, Hayashi H *et al.* Short-chain fatty acid receptor, GPR43, is expressed by enteroendocrine cells and mucosal mast cells in rat intestine. *Cell Tissue Res* 2006; **324**: 353–60.
19 Karaki SI, Tazoe H, Hayashi H *et al.* Expression of the short-chain fatty acid receptor, GPR43, in the human colon. *J Mol Histol* 2008; **39**: 135–42.
20 Bergman EN. Energy contributions of volatile fatty acids from the gastrointestinal tract in various species. *Physiol Rev* 1990; **70**: 567–90.
21 Le Poul E, Loison C, Struyf S *et al.* Functional characterization of human receptors for short chain fatty acids and their role in polymorphonuclear cell activation. *J Biol Chem* 2003; **278**: 25481–9.
22 Cummings JH, Pomare EW, Branch WJ, Naylor CP, Macfarlane GT. Short chain fatty acids in human large intestine, portal, hepatic and venous blood. *Gut* 1987; **28**: 1221–7.
23 Topping DL, Clifton PM. Short-chain fatty acids and human colonic function: roles of resistant starch and nonstarch polysaccharides. *Physiol Rev* 2001; **81**: 1031–64.
24 Key TJ, Allen NE, Spencer EA, Travis RC. The effect of diet on risk of cancer. *Lancet* 2002; **360**: 861–8.
25 Reif S, Klein I, Lubin F, Farbstein M, Hallak A, Gilat T. Pre-illness dietary factors in inflammatory bowel disease. *Gut* 1997; **40**: 754–60.

Supporting Information

Additional Supporting Information may be found in the online version of this article:

Table S1. Gallbladder cancer cDNA isolated from 3T3 transformants.

Please note: Wiley-Blackwell are not responsible for the content or functionality of any supporting materials supplied by the authors. Any queries (other than missing material) should be directed to the corresponding author for the article.

Cancer Science
The official journal of the Japanese Cancer Association

Identification of the transforming activity of Indian hedgehog by retroviral expression screening

Hisashi Hatanaka,[1,2] Shuji Takada,[1] Mamiko Tsukui,[2] Young Lim Choi,[1,4] Kentaro Kurashina,[3] Manabu Soda,[1] Yoshihiro Yamashita,[1] Hidenori Haruta,[1] Toru Hamada,[1] Kiichi Tamada,[2] Yoshinori Hosoya,[3] Naohiro Sata,[3] Hideo Nagai,[3] Yoshikazu Yasuda,[3] Kentaro Sugano[2] and Hiroyuki Mano[1,4,5,6]

Divisions of [1]Functional Genomics and [2]Gastroenterology, [3]Department of Surgery, Jichi Medical University, Tochigi; [4]Department of Medical Genomics, Graduate School of Medicine, The University of Tokyo, Tokyo; [5]CREST, Japan Science and Technology Agency, Saitama, Japan

(Received May 10, 2009/Revised August 29, 2009/Accepted September 2, 2009/Online publication September 30, 2009)

To identify novel cancer-promoting genes in biliary tract cancer (BTC), we constructed a retroviral cDNA expression library from a clinical specimen of BTC with anomalous pancreaticobiliary duct junction (APBDJ), and used the library for a focus formation assay with 3T3 fibroblasts. One of the cDNAs rescued from transformed foci was found to encode Indian hedgehog homolog (IHH). The oncogenic potential of IHH was confirmed both *in vitro* with the focus formation assay and *in vivo* with a tumorigenicity assay in nude mice. The isolated *IHH* cDNA had no sequence alterations, suggesting that upregulation of IHH expression may contribute to malignant transformation. Quantitation of *IHH* mRNA among clinical specimens has revealed that the expression level of *IHH* in BTC with APBDJ is higher than that in BTC without APBDJ and than in non-cancerous biliary tissues. Our data thus implicate a direct role of IHH in the carcinogenesis of BTC with APBDJ. (*Cancer Sci* 2010; 101: 60–64)

Biliary tract cancer (BTC) is a highly fatal malignancy in humans, and is prevalent in South American and Asian countries; approximately sixteen thousand people die of BTC every year in Japan.[1] Unfortunately, many BTC cases are diagnosed at advanced clinical stages with a 5-year survival rate of ~10%.[2–4] Several risk factors for BTC have been identified to date, including cholelithiasis,[5] anomalous pancreaticobiliary duct junction (APBDJ),[6] and primary sclerosing cholangitis.[7] Genetic alternations in *KRAS* or *TP53* and/or overexpression of *ERBB2* have been shown to contribute to the development of certain types of BTC. However, many cases with BTC do not harbor any such genetic changes, and other transforming events further await discovery.

The focus formation assay with 3T3 or RAT1 fibroblasts has been extensively used to screen for transforming genes in various carcinomas.[8] In such screening, genomic DNA is isolated from cancer specimens, and used to transfect 3T3 fibroblasts to obtain transformed cell foci. As expression of transfected genes in 3T3 cells in this assay is regulated by their own promoter and enhancer fragments, oncogenes with tissue-specific expression (e.g. those with a blood cell-specific promoter) can not become transcriptionally active in 3T3 cells, and thus can no longer be captured in such a screening system.

To ensure the sufficient expression of oncogenes in 3T3 cells, their transcription should be directly regulated by an exogenous promoter fragment. We have therefore constructed a retroviral cDNA expression library from a surgically operated clinical specimen of BTC with APBDJ, which was subsequently used to infect 3T3 cells. In the preparation of the cDNA library, we further took advantage of the SMART PCR system (Clontech, Mountain View, CA, USA), which preferentially amplifies full-length cDNA. A focus formation assay with the library has resulted in the identification of a transforming Indian hedgehog homolog (*IHH*) cDNA.

Materials and Methods

Focus formation assay with a retroviral library. A recombinant retroviral library was constructed as described previously,[9–12] with minor modifications. In brief, total RNA was extracted from a BTC specimen with APBDJ isolated from a 67-year-old man, who gave informed consent. This study was approved by the ethics committee of Jichi Medical University. First-strand cDNA was synthesized from the RNA with the use of PowerScript reverse transcriptase, the SMART IIA oligonucleotide, and CDS primer IIA (all from Clontech). The resulting cDNA was then amplified by PCR with 5′-PCR primer IIA (Clontech) and PrimeSTAR HS DNA polymerase (Takara Bio, Shiga, Japan) for 18 cycles of 98°C for 10 s and 68°C for 6 min. The PCR products were ligated to a *Bst*XI adapter (Invitrogen, Carlsbad, CA, USA) and then incorporated into the pMXS retroviral plasmid (kindly provided by T. Kitamura of the Institute of Medical Science, University of Tokyo). A total of 5.8×10^5 colony forming units of independent plasmid clones was thus generated. Twenty clones were randomly isolated from the library, and examined for the incorporated cDNA. Sixteen (80%) out of the 20 clones contained cDNA inserts with an average length of 1.16 kbp. Recombinant retroviruses were produced by introduction of the plasmid library into the packaging cell line BOSC23 (American Type Culture Collection, Manassas, VA, USA) and were used to infect 3T3 cells in the presence of 4 μg/mL polybrene (Sigma, St Louis, MO, USA). The cells were cultured for 2 weeks, after which transformed foci were isolated, expanded, and subjected to extraction of genomic DNA. Insert cDNA was recovered from the genomic DNA by PCR with 5′-PCR primer IIA and PrimeSTAR HS DNA polymerase. Amplified products were then ligated to the plasmid pT7Blue-2 (Novagen, Madison, WI, USA) and subjected to nucleotide sequencing.

Tumorigenicity assay in nude mice. 3T3 cells (2×10^6) were infected with a retrovirus expressing IHH, resuspended in 500 μL PBS, and injected into each shoulder of a *nu/nu* Balb-c mouse (6 weeks old). Tumor formation was assessed after 2 weeks.

Anchorage-independent growth in soft agar. 3T3 cells (2×10^6) were infected with a retrovirus encoding IHH or v-Ras, resuspended in the culture medium supplemented with 0.4% agar (Sea Plaque GTG agarose; Cambrex, East Rutherford, NJ, USA), and seeded onto a base layer of complete medium supplemented with 0.5% agar. Cell growth was assessed after culture for 2–3 weeks.

Quantitative RT-PCR analysis. Portions of oligo(dT)-primed cDNA produced by reverse transcription were subjected to PCR with a QuantiTect SYBR Green PCR kit (Qiagen, Valencia, CA, USA) and an amplification protocol comprising incubation at 94°C for 15 s, 60°C for 30 s, and 72°C for 60 s. Incorporation

[6]To whom correspondence should be addressed. E-mail: hmano@jichi.ac.jp

doi: 10.1111/j.1349-7006.2009.01355.x

of the SYBR Green dye into PCR products was monitored in real time with an ABI PRISM 7900HT sequence detection system (Applied Biosystems, Foster City, CA, USA), thereby allowing determination of the threshold cycle (C_T) at which exponential amplification of PCR products begins. The C_T values for cDNA corresponding to the β-actin gene (*ACTB*) and *IHH* were used to calculate the abundance of the latter mRNA relative to that of the former. The oligonucleotide primers used for PCR were 5′-CCATCATGAAGTGTGACGTGG-3′ and 5′-GTCCGCCTAGAAGCATTTGCG-3′ for *ACTB* and 5′-CCTCTCTCCTAGAGACCTTG-3′ and 5′-CTGGCTCCCAGGGAATTTAG-3′ for *IHH*.

Immunohistochemistry. Human tissues were fixed in 4% formaldehyde in PBS overnight at room temperature, embedded in paraffin, and sectioned at a thickness of 3 μm. Sections were mounted on glass slides, deparaffinized in three changes of xylene for 4 min each, and rehydrated in distilled water through a series of graded alcohols. For histological evaluation, sections were stained with hematoxylin–eosin. For immunohistochemical experiments, antigenicity was enhanced by boiling the sections in 10 mM citrate buffer (pH 6.0) in a microwave oven for 15 min, and the endogenous peroxidase activity was blocked by incubation in methanol containing 0.3% H_2O_2 for 30 min. After two washes with PBS containing 1% Triton X-100, the sections were preincubated with the blocking buffer (#X0909; Dako, Glostrup, Denmark) in a humidified chamber for 20 min at room temperature, and then incubated overnight at 4°C with anti-IHH antibody (sc-1196; Santa Cruz Biochemistry, Santa Cruz, CA, USA) diluted in PBS. Next, the sections were washed in PBS and incubated with horseradish peroxidase-labeled polymers conjugated to secondary antibodies for primary rabbit antigoat immunoglobulin (Dako, #P0449) without dilution at 37°C for 30 min. Color development was carried out by incubating the sections with 3,3-diaminobenzidine tetrahydrochloride (Wako Pure Chemical Industries, Osaka, Japan) as the chromogenic substrate. Finally, the sections were lightly counterstained with hematoxylin, mounted, and viewed under a light microscope. For the negative control, the immunostaining processes were carried out by replacing the primary antibody with PBS.

Results

Screening with the focus formation assay. From the mRNA of a BTC specimen with APBDJ, full-length cDNA was selectively amplified and ligated to a retroviral vector pMXS. From such library plasmids, we generated a recombinant ecotropic retrovirus that was subsequently used to infect mouse 3T3 fibroblasts. Infection experiments were repeated for a total of four times. After 3 weeks of culture, 75 transformed foci were observed. No foci could be found among the cells infected with an empty virus, while numerous foci were easily identified in the cells infected with a virus expressing v-Ras oncoprotein (data not shown).

Table 1. Bile duct cancer cDNA isolated from 3T3 transformants

Clone ID #	Gene symbol	GenBank no.	Presence of full ORF
1	*FAM83H*	NM_198488	No
2	*GATAD1*	NM_021167	Yes
3	*RRAS2*	NM_012250	No
4	*FASTK*	NM_006712	Yes
5	*VAT1*	NM_006373	Yes
6	*ARPC2*	NM_005731	No
7	*IHH*	NM_002181	Yes
8	*SENP6*	NM_015571	Yes
9	*DOT1L*	NM_032482	ND
10	*LTBR*	NM_002342	ND
11	*KRAS*	NM_004985	Yes
12	*TMEM54*	NM_033504	Yes
13	*RNASET2*	NM_003730	Yes
14	*RPS4X*	NM_001007	Yes
15	*TETRAN*	NM_001120	Yes
16	*DFNB31*	NM_015404	No
17	*CLDN3*	NM_001306	No
18	*GJB2*	NM_004004	Yes
19	*PSMA7*	NM_002792	Yes
20	*PRPSAP1*	NM_002766	Yes
21	*LRRC59*	NM_018509	Yes
22	*LRP5*	NM_002335	ND
23	*NCOR2*	NM_006312	No
24	*KLF16*	NM_031918	No
25	*ARHGAP4*	NM_001666	ND
26	*KIAA0284*	NM_015005	No
27	*DNAJC4*	NM_005528	ND
28	*NOTCH2NL*	NM_203458	No
29	*BCKDHB*	NM_000056	Yes

ND, not determined; ORF, open reading frame.

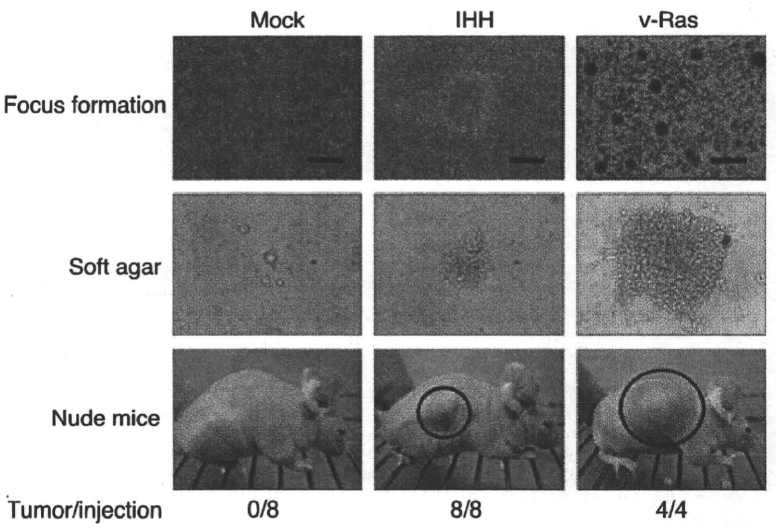

Fig. 1. Transforming activity of Indian hedgehog homolog (IHH). Mouse 3T3 cells were infected with viruses encoding IHH or v-Ras or with the empty virus (Mock), and were then cultured for 5 days for the analysis of focus formation (top panels; scale bars = 1 mm). The same batches of 3T3 cells were also assayed for anchorage-independent growth in soft agar over 17 days (middle panels) and for tumorigenicity in nude mice over 3 weeks (bottom panels). Tumors formed in the shoulders of mice injected subcutaneously with 1×10^5 cells are indicated by red circles. The frequency of tumor formation (tumors/injection) is also indicated.

Each focus was isolated, expanded independently, and used to prepare genomic DNA. We then tried to recover retroviral inserts from such genomic DNA by PCR amplification with the primer used originally to amplify the cDNA in the construction of the library. In most cases, one to three DNA fragments were recovered from each genome, implying multiple retroviral infection of some 3T3 cells.

We finally obtained a total of 44 cDNA fragments by PCR, each of which was ligated into a cloning vector, and subjected to nucleotide sequencing from both ends. Screening of the 44 cDNA sequences against the public nucleotide sequence databases revealed that the 44 fragments correspond to 29 independent genes (Table 1).

Identification of IHH. To confirm the transforming potential of the isolated cDNA, each cDNA clone was ligated to pMXS, and corresponding retrovirus was used to re-infect 3T3 cells. Focus formation assays were conducted for 13 independent genes, discovering a reproducible transforming activity for clone ID #7 corresponding to *IHH* (GenBank accession number, NM_002181) (Fig. 1, top panel). Again, infection with a virus for v-Ras induced many transformed foci, while an empty virus failed to do so. The entire coding region of our ID #7 cDNA was sequenced, revealing no point mutations or deletions compared to the published *IHH* cDNA sequence. Although activation of Hedgehog (Hh) pathways has been revealed among a wide range of digestive tract cancers,[13] oncogenic activity of *IHH* has not been reported to date. We supposed from our data that overexpression of *IHH* may contribute directly to malignant transformation.

Confirmation of the transforming activity of IHH. To confirm the oncogenic activity of IHH, we examined its effect on the anchorage-independent growth of 3T3 cells in soft agar. Whereas cells infected with an empty virus did not grow in the agar, those infected with a virus expressing IHH formed multiple foci in repeated experiments (Fig. 1, middle panel). In addition, 3T3 cells expressing v-Ras readily grew in the agar.

The transforming activity of IHH was also tested by the tumor formation assay with athymic nude mice. 3T3 cells infected with the empty virus or retrovirus expressing IHH or v-Ras were inoculated subcutaneously into nude mice. As shown in the bottom panel of Fig. 1, tumor formation was readily observed for the cells expressing IHH or v-Ras. These results clearly revealed

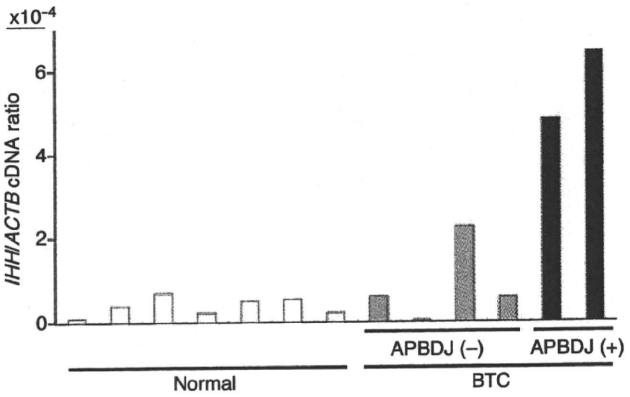

Fig. 2. Expression of Indian hedgehog homolog (*IHH*) in biliary tract. Oligo(dT)-primed cDNA was synthesized from clinical specimens of biliary tract cancer (BTC) with (+) or without (−) anomalous pancreaticobiliary duct junction (APBDJ), or from normal gallbladder (Normal), and were subjected to quantitative PCR analysis for cDNA of *IHH* and β-actin (*ACTB*). The relative expression level of the former to the latter is represented.

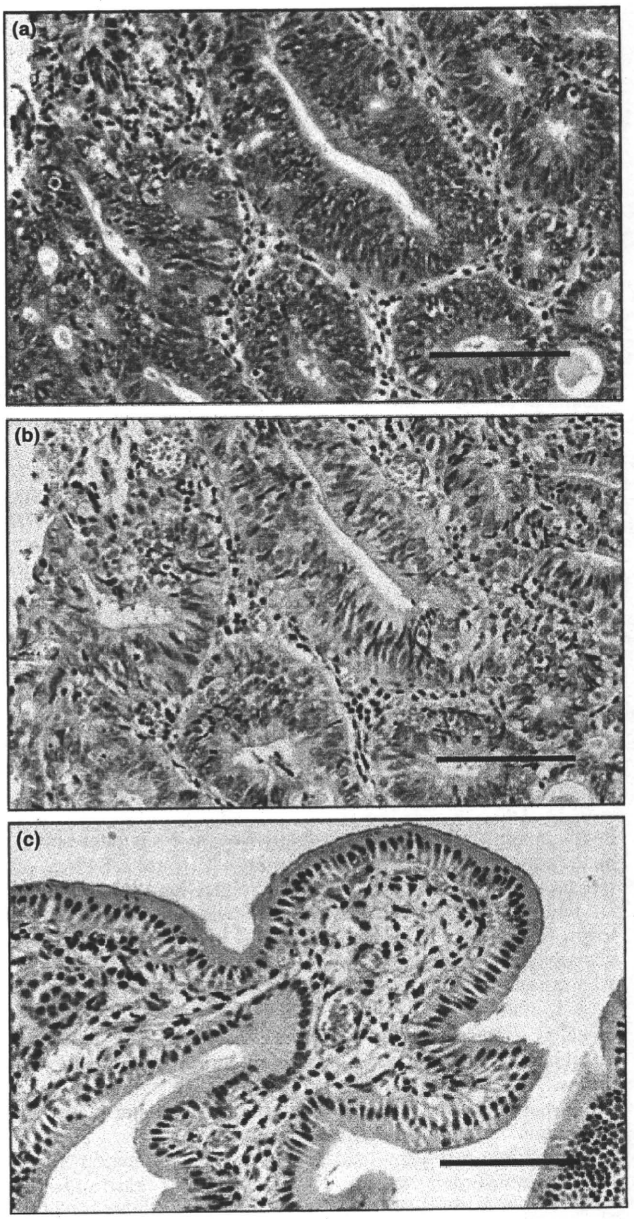

Fig. 3. Immunohistochemical detection of Indian hedgehog homolog (IHH). Expression of IHH is elevated in (a) biliary tract cancer with anomalous pancreaticobiliary duct junction, but such reactivity was absent in the control experiment for (b) the same specimen or (c) anti-IHH staining in normal gallbladder. Scale bars = 100 μm.

an unexpected, direct transforming potential of IHH in fibroblasts.

Overexpression of *IHH* mRNA. Given the transforming potential of wild-type IHH (when it is abundantly expressed), we tried to examine if *IHH* is overexpressed in BTC specimens. Real-time RT-PCR analysis for the quantitation of *IHH* cDNA among normal gall bladder ($n = 7$) and BTC specimens ($n = 6$) (Supporting Information Table S1) revealed that *IHH* is indeed overexpressed in the latter specimens, albeit with marginal statistical significance ($P = 0.06$) by a two-tailed t-test (Fig. 2). It should be noted, however, that BTC cases with APBDJ ($n = 2$) had significantly abundant expression of *IHH* compared to BTC

doi: 10.1111/j.1349-7006.2009.01355.x

without APBDJ ($P = 0.005$) or to normal gall bladder ($P = 2.4 \times 10^{-6}$). Therefore, it is likely that some types of BTC overexpress IHH.

Protein expression of IHH. To confirm the elevated expression of IHH in BTC, we examined its protein level by an immunohistochemical approach. In accordance with the RT-PCR experiments, IHH protein was abundantly detected only in the cytoplasm of cancerous duct but not in stromal cells for BTC with APBDJ (Fig. 3). We failed to observe such staining in normal gallbladder, suggesting that IHH protein was markedly induced in BTC with APBDJ compared to normal gallbladder.

Discussion

In the present study, we have constructed a retroviral cDNA expression library for a BTC specimen with APBDJ, and unexpectedly revealed the transforming potential of IHH through a focus formation assay with the mouse fibroblast cell line 3T3. As there were no sequence alterations in our isolated *IHH* cDNA, the high expression of IHH is likely to exert its oncogenic activity. Consistent with this notion, expression of *IHH* was indeed activated in BTC with APBDJ.

In our transformation assays for IHH (i.e. focus formation assay, soft agar-growth assay, and nude mouse-tumorigenicity assay) we directly used a highly polyclonal, mass culture of 3T3 cells infected with a retrovirus expressing IHH, without any selection (such as positive selection for neomycin resistance-cells). Repeated confirmation of the transforming potential for IHH in such assays (and not for an empty virus) strongly argues against a hypothesis that an artificial expression of mouse genes adjacent to the retroviral integration sites was responsible for the 3T3 transformation in these experiments.

The Hh signaling pathway was originally described in the development of *Drosophila melanogaster* as a segment polarity gene required for embryonic patterning.[14] There are three vertebrate homologues of Hh: Ihh, Sonic hedgehog (Shh), and Desert hedgehog (Dhh) with similar biological properties among them. Hh signaling is known to play a pivotal role in cell fate decisions,[15] tissue repair,[16] and stem cell self renewal.[17,18] Aberration in such signaling may contribute to sustained cell growth and cancer. Indeed, Hahn *et al.* and Johnson *et al.* revealed that mutations within *PTCH1* (a binding partner of hedgehog) cause a cancer-promoting condition, Gorlin syndrome.[19,20] Further, frequent mutations in Hh signaling components have also been identified among sporadic basal cell carcinoma[21] and medulloblastoma.[22]

In addition, transcriptional activation of Hh components has been demonstrated among a wide range of gastrointestinal tumors, which results from endogenous overexpression of Hh proteins such as IHH and SHH.[13] Despite the lack of gene mutations for the Hh components in these tumors, cyclopamine, a specific inhibitor for SMO, suppresses the growth of tumors positive for elevated Hh signaling, supporting the idea that overexpression of the Hh family of proteins may have a mitogenic function.

Our current data proves for the first time the direct transforming potential of IHH, at least in fibroblasts. Furthermore, apparent overexpression of *IHH* in BTC with APBDJ indicates an important role of IHH especially in this subtype of BTC. In addition to the presence or absence of APBDJ, we also examined the clinicopathological features of the BTC specimens used in our study. As shown in Supporting Information Table S1, none of the TNM stage, clinical stage, KRAS mutation, or Ki-67 index were related to the overexpression of *IHH*. However, because the current cohort size is still small, a larger cohort study is mandatory to examine the clinical features of BTC with high *IHH*.

Although Yang *et al.* reported that treatment with a SMO inhibitor leads to downregulation of *CCND1* and upregulation of *CDKN1A* in a cell line of pancreatic carcinoma,[23] we did not observe such a relationship between *CCND1/CDKN1A* and *IHH* expression (data not shown). However, overexpression of *CCND1* may be more prevalent among BTC than that of *IHH*,[24] suggesting the presence of an IHH-independent regulatory network for *CCND1* in BTC.

APBDJ causes pancreatic fluid regurgitation into the biliary duct, and is found frequently among BTC cases.[25] Because pancreatic fluid is rich in various proteases, frequent regurgitation of such fluid into the biliary tract is likely to cause sustained inflammation in the tract. Because inflammation and tissue repair cause transcriptional activation of the Hh family of soluble factors,[16] it may not be surprising to find an elevated level of *IHH* mRNA in the biliary tract with APBDJ. Given the transforming function of abundant IHH, such overexpression may lead to increased cell cycle of biliary tract cells, and eventually to the generation of BTC. Because a number of chemical inhibitors are under development for the Hh pathways,[26] BTC with APBDJ would be an intriguing candidate for such drugs. Further, it is also tempting to examine the Hh ligand levels among human cancers associated with chronic inflammation or regeneration.

Acknowledgments

This work was supported in part by grants for Research on Human Genome and Tissue Engineering and for Third-Term Comprehensive Control Research for Cancer from the Ministry of Health, Labor, and Welfare of Japan, as well as by a grant for Scientific Research on Priority Areas "Applied Genomics" from the Ministry of Education, Culture, Sports, Science, and Technology of Japan.

Abbreviations

CCND1	cyclin D1
CDKN1A	cyclin-dependent kinase inhibitor 1A
ERBB2	v-erb-b2 avian erythroblastic leukemia viral oncogene homolog 2
KRAS	v-ki-ras2 Kirsten rat sarcoma viral oncogene homolog
PTCH1	Patched, Drosophila, homolog of, 1
TP53	tumor protein p53

References

1 National Cancer Center. *Cancer statistics in Japan 2007 (Website on the internet)*. Tokyo, Japan: National Cancer Center, 2008. [Cited 16 November 2007.] Available from URL: http://www.ganjoho.jp/public/statistics/backnumber/2007_en.html.

2 Carriaga MT, Henson DE. Liver, gallbladder, extrahepatic bile ducts, and pancreas. *Cancer* 1995; **75**: 171–90.

3 Cubertafond P, Gainant A, Cucchiaro G. Surgical treatment of 724 carcinomas of the gallbladder. Results of the French Surgical Association Survey. *Ann Surg* 1994; **219**: 275–80.

4 Shaib Y, El-Serag HB. The epidemiology of cholangiocarcinoma. *Semin Liver Dis* 2004; **24**: 115–25.

5 Zatonski WA, Lowenfels AB, Boyle P *et al.* Epidemiologic aspects of gallbladder cancer: a case-control study of the SEARCH Program of the International Agency for Research on Cancer. *J Natl Cancer Inst* 1997; **89**: 1132–8.

6 Hasumi A, Matsui H, Sugioka A *et al.* Precancerous conditions of biliary tract cancer in patients with pancreaticobiliary maljunction: reappraisal of nationwide survey in Japan. *J Hepatobiliary Pancreat Surg* 2000; **7**: 551–5.
7 Rosen CB, Nagorney DM, Wiesner RH, Coffey RJ Jr, LaRusso NF. Cholangiocarcinoma complicating primary sclerosing cholangitis. *Ann Surg* 1991; **213**: 21–5.
8 Aaronson SA. Growth factors and cancer. *Science* 1991; **254**: 1146–53.
9 Soda M, Choi YL, Enomoto M *et al.* Identification of the transforming *EML4–ALK* fusion gene in non-small-cell lung cancer. *Nature* 2007; **448**: 561–6.
10 Hatanaka H, Takada S, Choi YL *et al.* Transforming activity of purinergic receptor P2Y, G-protein coupled, 2 revealed by retroviral expression screening. *Biochem Biophys Res Commun* 2007; **356**: 723–6.
11 Fujiwara S, Yamashita Y, Choi YL *et al.* Transforming activity of purinergic receptor P2Y, G protein coupled, 8 revealed by retroviral expression screening. *Leuk Lymphoma* 2007; **48**: 978–86.
12 Choi YL, Kaneda R, Wada T *et al.* Identification of a constitutively active mutant of JAK3 by retroviral expression screening. *Leuk Res* 2007; **31**: 203–9.
13 Berman DM, Karhadkar SS, Maitra A *et al.* Widespread requirement for Hedgehog ligand stimulation in growth of digestive tract tumours. *Nature* 2003; **425**: 846–51.
14 Nusslein-Volhard C, Wieschaus E. Mutations affecting segment number and polarity in Drosophila. *Nature* 1980; **287**: 795–801.
15 Ingham PW, McMahon AP. Hedgehog signaling in animal development: paradigms and principles. *Genes Dev* 2001; **15**: 3059–87.
16 Beachy PA, Karhadkar SS, Berman DM. Tissue repair and stem cell renewal in carcinogenesis. *Nature* 2004; **432**: 324–31.
17 Liu S, Dontu G, Wicha MS. Mammary stem cells, self-renewal pathways, and carcinogenesis. *Breast Cancer Res* 2005; **7**: 86–95.
18 Liu S, Dontu G, Mantle ID *et al.* Hedgehog signaling and Bmi-1 regulate self-renewal of normal and malignant human mammary stem cells. *Cancer Res* 2006; **66**: 6063–71.
19 Hahn H, Wicking C, Zaphiropoulous PG *et al.* Mutations of the human homolog of Drosophila patched in the nevoid basal cell carcinoma syndrome. *Cell* 1996; **85**: 841–51.
20 Johnson RL, Rothman AL, Xie J *et al.* Human homolog of patched, a candidate gene for the basal cell nevus syndrome. *Science* 1996; **272**: 1668–71.
21 Reifenberger J, Wolter M, Weber RG *et al.* Missense mutations in SMOH in sporadic basal cell carcinomas of the skin and primitive neuroectodermal tumors of the central nervous system. *Cancer Res* 1998; **58**: 1798–803.
22 Taylor MD, Liu L, Raffel C *et al.* Mutations in SUFU predispose to medulloblastoma. *Nat Genet* 2002; **31**: 306–10.
23 Yang Y, Tian X, Xie X, Zhuang Y, Wu W, Wang W. Expression and regulation of hedgehog signaling pathway in pancreatic cancer. *Langenbecks Arch Surg* 2009; doi. 10.1007/s00423-009-0493-9.
24 Hui AM, Li X, Shi YZ, Takayama T, Torzilli G, Makuuchi M. Cyclin D1 overexpression is a critical event in gallbladder carcinogenesis and independently predicts decreased survival for patients with gallbladder carcinoma. *Clin Cancer Res* 2000; **6**: 4272–7.
25 Kimura K, Ohto M, Saisho H *et al.* Association of gallbladder carcinoma and anomalous pancreaticobiliary ductal union. *Gastroenterology* 1985; **89**: 1258–65.
26 Rubin LL, de Sauvage FJ. Targeting the Hedgehog pathway in cancer. *Nat Rev Drug Discov* 2006; **5**: 1026–33.

Supporting Information

Additional Supporting Information may be found in the online version of this article:

Table S1. Clinical characteristics of the patients with biliary tract cancer (BTC).

Please note: Wiley-Blackwell are not responsible for the content or functionality of any supporting materials supplied by the authors. Any queries (other than missing material) should be directed to the corresponding author for the article.

doi: 10.1111/j.1349-7006.2009.01355.x

INTERNAL MEDICINE

□ ORIGINAL ARTICLE □

Clinical Features of Lymphangioleiomyomatosis Complicated by Renal Angiomyolipomas

Yoshiko Mizushina, Masashi Bando, Tatsuya Hosono, Naoko Mato, Takakiyo Nakaya, Yoshikazu Ishii, Hideaki Yamasawa and Yukihiko Sugiyama

Abstract

Objective Renal angiomyolipomas (R-AMLs) are major complications of lymphangioleiomyomatosis (LAM). The objective of this study was to better understand the influence of R-AMLs in patients with LAM on the prognosis and other clinical factors related to respiration, and to investigate the management of R-AMLs in patients with LAM.

Patients and Methods We retrospectively investigated the clinical features of 7 patients with LAM [4 were TSC (Tuberous sclerosis complex)-LAM and 3 were S (sporadic)-LAM] complicated by R-AMLs admitted to our hospital from 1997 to 2008.

Results All patients were females and the mean age at diagnosis of LAM was 40.7 years (31.7 years for TSC-LAM and 52.7 years for S-LAM). Although 5 patients had symptoms related to R-AMLs, only 1 patient experienced symptoms related to R-AMLs at the time of diagnosis. Five patients had bilateral and 2 patients had unilateral R-AMLs. R-AMLs ruptured in 4 cases (3 patients were TSC-LAM) including 2 patients in whom they ruptured bilaterally, and who underwent bilateral nephrectomy. In 1 case, unilateral R-AMLs grew larger and appeared on the other side during the follow-up period.

Conclusion Although only rare cases of LAM show symptoms related to R-AMLs initially, R-AMLs are a notable complication. To avoid nephrectomy, R-AMLs should be diagnosed when they are small and should be followed up carefully by periodic echograms or CT scans.

Key words: lymphangioleiomyomatosis, renal angiomyolipoma, tuberous sclerosis complex, total nephrectomy

(Intern Med 50: 285-289, 2011)
(DOI: 10.2169/internalmedicine.50.3558)

Introduction

Lymphangioleiomyomatosis (LAM) is a rare disease that occurs predominantly in females and is characterized by the proliferation of smooth muscle cells and cyst formation. LAM occurs in 30% of patients with tuberous sclerosis complex (TSC), but patients with LAM complicated by TSC (TSC-LAM) constitute only approximately 15% of all LAM cases. The remaining cases are sporadic LAM (S-LAM). LAM patients have renal angiomyolipomas (R-AMLs) in about 93% of TSC-LAM and about 30-50% of S-LAM cases (1).

In order to better understand the influence of R-AMLs in patients with LAM on the prognosis and other clinical factors related to respiration, and to investigate the management of R-AMLs in patients with LAM, we retrospectively investigated 7 cases of LAM complicated by R-AMLs who were admitted to our hospital from 1997 to 2008.

Patients and Methods

Thirteen patients with LAM were admitted to our hospital from 1977 to 2008. We investigated the clinical features of 7 patients with LAM (4 were TSC-LAM and 3 were S-LAM) complicated by R-AMLs. Retrospective chart reviews were performed on each case. The size of the R-AMLs were measured from echograms or computed tomography (CT)

Division of Pulmonary Medicine, Department of Medicine, Jichi Medical University, Japan
Received for publication February 18, 2010; Accepted for publication October 11, 2010
Correspondence to Dr. Yoshiko Mizushina, mizushina@jichi.ac.jp

Table 1. Clinical Characteristics of 13 LAM Cases

Case No.	Age of diagnosis as LAM*1	Age of initial symtoms	R-AMLs *2	TSC *3	Initial symtoms	Symptoms of R-AMLs	Pneumothorax	Duration until induction of HOT*4 from initial symptoms[years]	Decline of VC*5/year[ml]	Decline of $FEV_{1.0}$*6/year[ml]	Therapy	Follow up period from diagnosis	Respiratory failure
1	32	27	+	-	Chest pain	Abdominal pain	+	-			progesteron	26 years	-
2	58	50	+	-	Dyspnea on exertion	Abdominal pain	+	11	12.86	51.43		Induction of IPPV for respiratory failure after 9 years	+
3	42	41	+	-	Dyspnea on exertion	-	-	13	1.54	52.31	progesteron	Progression of respiratory failure Transfer to another hospital after 16 years	+
4	34	32	+	+	Dyspnea on exertion	Abdominal pain and lumbago	+	3	136.67	79.17	progesteron	Progression of respiratory failure 14 years	+
5	29	29	+	+	Cough and fever	Appetite loss and nausea	-	-	-5.00	-21.67		Induction of hemodialysis 15 years	-
6	58	30	+	-	Pneumothorax	-	+	2				Dead of respiratory failure after 2 years Diagnosed by autopsy	+
7	32	31	+	+	Abdominal distention	Abdominal distention	+	-				2 years Renal transplantation was performed	-
8	42	39	-	-	Hemosputum		+	-	25.00	24.29		Progression of respiratory failure Dead of breast cancer after 17 years	+
9	46	40	-	-	Dyspnea on exertion		-	-				Dead of respiratory failure after 2 years Diagnosed by autopsy	+
10	38	37	-	-	Back pain		+	-	41.88	42.50		17 years	-
11	33	32	-	-	Cough and sputum		-	5	58.89	26.67	Progesteron +ovariectomy	Induction of IPPV for respiratory failure after 14 years	+
12	29	29	-	-	Cough and fever		-	-			progesteron	Drainage of chylothorax Transfer to another hospital after a year	-
13	29	27	-	-	Cough and lumbago		-	2	477.50	137.50	Progesteron LH-RH analog, Lung transplantation	Lung transplantation was performed after 3 years 3 years after transplantation	+

*1 LAM; Lymphangioleiomyomatosis, *2 R-AML; renal angiomyolipoma, *3 TSC; Tuberous sclerosis complex
*4 HOT; Home oxygen therapy, *5 VC; Vital capacity, *6 $FEV_{1.0}$; Forced expiratory volume in 1 second,

scans.

We diagnosed LAM using the diagnostic criteria established by the Respiratory Failure Research Group of the Japanese Ministry of Health, Labour and Welfare in 2005 (2).

We diagnosed R-AMLs based on echograms or CT scans. The appearance of R-AMLs on echogram is a strongly hyper-reflective lesion with acoustic shadowing. This appearance is a result of the multiple tissue interfaces between fatty and non-fatty components of the mass. The appearance of R-AMLs on unenhanced CT scan is a predominantly fatty inhomogeneous mass with varying amounts of tissue density interspersed within it. Minimal fat AMLs which contain only microscopically detectable fat account for 4.5% of R-AMLs. Although it is difficult to diagnose minimal fat AMLs by their appearance on echogram or CT scan, homogeneous enhancement and a prolonged enhancement pattern on CT scan are the most accurate predictors (3).

A statistical software package (Dr.SPSS II, for Windows; SPSS Inc.) was used for the analysis. Results are presented as the mean±standard error of the mean (SEM). The differences between the two groups were compared using Student's unpaired t-test. Fisher's exact test was calculated to assess relationships between the two parameters. A value of $p<0.05$ was considered statistically significant.

Case 7 was previously reported in 2008 in *Urology* (4).

Results

All of the patients were females and the mean age at diagnosis of LAM was 40.7 years. Seven cases were complicated by R-AMLs (Table 1).

All 4 patients (100%) with TSC-LAM had R-AMLs. Three of 9 patients (33%) with S-LAM had R-AMLs. The mean ages of patients at diagnosis of LAM with R-AMLs were 31.7 years for TSC-LAM patients and 52.7 years for S-LAM patients (Table 1). There were no significant differences between the groups with and without R-AMLs in the rates of pneumothorax ($p=0.21$) or respiratory failure ($p=0.63$).

Five patients had bilateral and 2 patients had unilateral R-AMLs. R-AMLs ruptured in 4 cases (3 patients were TSC-LAM), including 2 patients in whom they ruptured bilaterally. Renal artery embolization had been performed in 1 case, nephrectomy had been performed in 4 cases, and bilateral nephrectomy had been performed in the 2 cases with bilateral rupture (Table 2). Regarding changes in R-AMLs during the follow-up period, in 1 case (Case 1), unilateral R-AMLs grew larger (3 cm to 4 cm in 2 years) and appeared on the other side as well (Table 2). Four patients had hepatic angiomyolipomas and R-AMLs (3 were S-LAM and 1 was TSC-LAM) (Table 2).

Table 2. Clinical Course of 7 LAM Cases Complicated by Renal Angiomyolipomas

Case No.	R-AML*1	Size of R-AML	Rupture of R-AMLs	Intervention	Hepatic AML
1	Bilateral	Left 3→4cm; Right 0.5cm (2 years later)	-	Left nephrectomy	-
2	Left	Left 7×4cm	-		+
3	Bilateral	Left 0.5, 1and 3cm; Right 1cm	-		+
4	Bilateral	bilateral multiple 1-3cm nodules	Right	Arterial embolization	-
5	Bilateral	Left 8cm; Right 16cm	Bilateral	Bilateral nephrectomy	-
6	Left	Left 3cm(autopsy)	Left	Left nephrectomy	+
7	Bilateral	Left 36cm; Right 22cm	Bilateral	Bilateral nephrectomy	+

*1 R-AML; renal angiomyolipoma

Figure 1. Giant bilateral renal angiomyolipomas in abdominal computed tomography (Case 7). Giant bilateral renal angiomyolipomas are shown in abdominal computed tomography. A hepatic angiomyolipoma is also shown. The patient experienced abdominal distention which was a symptom related to renal angiomyolipomas at the time of diagnosis.

Five patients visited our hospital due to respiratory symptoms (3 were dyspneic on exertion and 2 had symptoms related to pneumothorax) (Table 1). Although 5 patients had symptoms related to R-AMLs, only 1 patient (Case 7) experienced symptoms related to R-AMLs at the time of diagnosis (Fig. 1) (4).

We investigated the mean survival time, decline of vital capacity (VC) and decline of forced expiratory volume in 1 second ($FEV_{1.0}$). In the R-AMLs group, the mean survival time, decline of VC per year and decline of $FEV_{1.0}$ per year were 23.33±3.55 years, 36.5±67.1 mL and 40.3±43.2 mL, respectively. On the other hand, in the no R-AMLs group, the mean survival time, decline of VC per year and decline of $FEV_{1.0}$ per year were 14.20±2.50 years, 150.8±218.2 mL and 57.7±53.8 mL, respectively. There were no significant differences between the 2 groups in these 3 parameters (p=0.66, p=0.09 and p=0.65, respectively).

Discussion

In the present study, 4 patients (100%) with TSC-LAM and 3 patients (33.3%) with S-LAM had R-AMLs. These results were compatible with those in previous reports showing that patients with LAM have R-AML in approximately 93% of TSC-LAM cases and 30-50% of S-LAM cases (1). In this study, although 5 patients showed symptoms related to R-AMLs, only 1 patient experienced symptoms related to R-AMLs at the time of diagnosis (4). The symptoms were relatively atypical at the time of diagnosis and might delay diagnosis. Therefore, this case is very important if we consider the history of LAM. The Respiratory Failure Research Group of the Japanese Ministry of Health, Labour and Welfare 2003-2004 reported on the epidemiology of LAM in Japan (5). In the report, 173 patients with LAM showed common presenting features of pneumothorax (43%), dyspnea on exertion (36%), abnormal shadow on chest radiograph (11%) and other respiratory symptoms (4%) such as haemoptysis, cough and chest pain. In contrast, only 6% of patients presented with abdominal manifestations attributable to LAM or R-AMLs (5). In Japan, although 12 cases with LAM complicated by R-AMLs have been reported previously (6-9), symptoms and diagnosis related to R-AMLs preceded the other symptoms in only 2 cases. The other 10 cases showed initial symptoms related to respiration. Pa-